Wind Turbine Entry and Transmission Expansion: Evaluating Spatial Subsidies in Germany

Pascal Heid

November 9, 2026

Click here for the most recent version

Abstract

Ambitious renewable energy targets create a costly spatial mismatch between electricity supply and demand under network constraints. I study how two policy margins interact in addressing the costs from balancing supply and demand: spatial renewable subsidy design that reduces the mismatch and transmission investment that relaxes network constraints but arrives with a delay. I develop and estimate a spatial model of onshore wind-turbine entry and combine it with a network-constrained dispatch model of the German electricity system allowing for endogenous congestion management. Removing the spatial signal from current subsidies leaves congestion and the benefits of a planned network expansion largely unchanged. Replacing the existing signal with a local congestion signal instead improves wind integration and lowers costs. On its own, this design achieves 26 percent of the gains from costly network expansion, substantially reducing incentives to undertake it.

1 Introduction

The green energy transition shifts electricity generation toward resource-rich areas that are often imperfectly interconnected with major electricity demand centers. This creates a costly spatial mismatch between supply and demand because binding transmission constraints make the least-cost solution to energy generation infeasible. Policymakers have three major options to alleviate these costs: expand transmission capacity to the resource-rich areas, incentivize generation in better-connected locations or combine both. This policy challenge arises worldwide and is particularly apparent in the European Union (EU). Grid operators plan to invest roughly EUR 72 billion per year through 2030 in transmission and distribution infrastructure (European Court of Auditors, 2025). Transmission expansion takes time, however, and the rapid growth of geographically concentrated and intermittent renewable generation is already straining existing networks, highlighting imperfect interconnection. Congestion management cost the EU EUR 4.2 billion in 2023, of which Germany accounted for approximately 60 percent (European Union Agency for the Cooperation of Energy Regulators, 2024).

This paper evaluates how spatial subsidy design affects the geography of wind turbine entry, how it endogenously changes the cost of managing transmission constraints until the grid can expand and how it alters incentives to invest in the grid. I therefore answer the question of how two policy margins—the spatial design of renewable support and delayed transmission expansion—interact in reducing the costly spatial mismatch between energy supply and demand while accommodating a large wind energy build-out.

I study this interaction empirically by combining a spatial entry model of German onshore wind turbines with a network-constrained electricity dispatch model allowing for endogenous management of transmission constraints. The two components are linked by translating the spatial allocation of wind turbines into electricity generation using data on turbine technology and local wind conditions. This novel combination allows me to quantify how changes in spatial subsidy design affect the geography of wind investment, how the resulting generation is accommodated by the transmission network, and how these changes affect generation and costs from binding network constraints. Explicitly modeling the physical transmission network further allows me to evaluate how the same allocation of wind turbines performs before and after grid expansion.

For the entry model, I use project-level data on all onshore wind turbines entering between 2004 and 2023, including their exact location, turbine technology, installed capacity, and commissioning year. Building on the renewable entry model of Gonzales et al. (2023), I allow for heterogeneous turbine technology and persistent differences in entry costs across regions and cohorts. I aggregate wind projects to the county–cohort level and estimate an entry equation relating installed wind capacity to expected discounted lifetime revenue, controlling for region and entry-cohort fixed effects in a two-way fixed effects model. Revenue is constructed based on the projects that were actually developed, including their exact sites and technologies. Developers select these based on unobserved local development conditions raising potential endogeneity concerns. I address this issue

by constructing an instrument based on potential revenue at the stage of choosing a county-cohort but before the precise turbine model and site are selected. The instrument provides identification under the assumption that shocks are unanticipated at the stage of choosing the county and cohort of entry. I consequently use instrumental variable estimation to recover the reaction of entry to changes in lifetime revenue.

For the dispatch model, I divide Germany into four zones corresponding to the regions served by its four transmission system operators (TSOs). I represent the observed transmission lines connecting these zones and their physical properties, allowing for transmission constraints between but not within TSO regions. Building on the network-constrained dispatch framework of Bohn et al. (1984) and Arkolakis and Walsh (2023), I incorporate endogenous measures for alleviating binding transmission constraints following the institutional sequence of the German wholesale electricity market. I simulate the model using data on electricity demand, renewable and conventional generation, imports, generation availability, and marginal costs. In the first stage, the national market minimizes generation costs with gross renewable generation and without transmission constraints. In the second stage, system operators adjust the initial generation schedule to accommodate grid constraints. This involves redispatch, which shifts conventional electricity generation between locations, and curtailment, which reduces wind generation when it cannot be accommodated by the network. Both arise from transmission congestion and capture the additional costs of balancing supply and demand under network constraints. I validate the dispatch model against observed redispatch and curtailment data for Germany in 2023.

I use this empirical framework to evaluate three spatial renewable subsidy designs under the same cohort-specific budget constraint, before and after a planned grid expansion. Under the status quo, subsidies are adjusted according to local wind productivity, with lower productivity leading to higher support. I compare this policy with two alternative subsidy rules: a geographically flat subsidy often simply called flat subsidy in the paper and a subsidy adjusted by lagged locational marginal prices which I call congestion-adjusted subsidy. The flat subsidy mimics free entry under a common guaranteed support level. This is because the German electricity market operates under one national bidding zone which means that there is a single national wholesale electricity price equivalent to the price derived from generation in the first stage outlined above. The congestion-adjusted subsidy instead incentivizes wind turbine entrants to take the system value of their location choice into account. It exposes wind turbine entrants to wind-generation-weighted average lagged prices derived from least-cost generation under network constraints, i.e. lagged locational marginal prices (LMPs) corrected for when wind energy is actually generated. This is an approximation to switching the German electricity system to nodal pricing with four nodes based on the four TSOs. Instead of changing the whole market design I only expose wind turbine operators to the average relative difference in nodal prices explicitly accounting for the fact that wind generation concentrates in hours when these differences are large. Under each subsidy rule the estimated entry model first determines where wind investment locates, after which the dispatch model maps this into generation,

redispatch and curtailment costs. I then add four major north–south high-voltage direct current (HVDC) transmission lines — planned in the early 2010s and projected to be operational starting 2026 — to the observed network and operate each wind allocation on the expanded grid. The model therefore quantifies both how subsidy-induced spatial entry affects transmission congestion before the grid adjusts and how it changes the benefits of subsequent transmission investment.

The paper has three main results. First, the counterfactuals show how subsidy design changes the geography of wind entry. Under the status quo, most of the onshore wind energy capacity is installed in the windy north of Germany close to the coast. Moving to a spatially flat support exacerbates this tendency shifting investment even more toward the most productive wind locations in the northern and coastal regions but also towards windier sites in the middle of the country. Congestion-adjusted support shifts entry away from locations with low marginal system value and toward higher-value parts of the grid. It increases northern investment where wind productivity remains sufficiently high while mainly inducing entry close to demand centers in the southwest and west of the country where the system-value is large.

Second, on the existing grid, flat support raises electricity-system cost by EUR 94 million annually relative to the status quo which is equivalent to 7 percent of the EUR 1.4 billion spent on onshore wind turbine support in 2023. Only ten percent of this cost increase is driven by larger congestion while the rest comes from lower total capacity under the flat subsidy outweighing the effect from entry into relatively more productive sites. This finding reveals a limitation of the current spatial subsidy design: at the four-TSO level, its wind-productivity adjustment provides little congestion relief relative to free entry under a common support level. Congestion-adjusted support removes this limitation. On the existing grid, it lowers total modeled electricity-system cost by EUR 166 million annually or by 12 percent of spending on onshore wind turbine support in 2023. A spatial signal but much more a congestion signal is important for keeping system costs low during the transition, when wind investment can respond well before transmission capacity is expanded. This is because the grid is already significantly congested and wind turbine geography contributes to it.

Third, adding the planned grid expansion demonstrates that the value of the same transmission investment depends on the wind geography created by the subsidy design. Without any grid expansion, congestion-adjusted support achieves roughly 26 percent of the cost reduction obtained by combining the status quo subsidy with the planned grid investment. Congestion-adjusted subsidies and network expansion therefore demonstrate a significant degree of substitutability. Because part of the spatial mismatch is already removed before transmission is expanded, the grid expansion is just cost-covering under congestion-adjusted support while the benefit-to-cost ratio is 1.52 under the status quo. This interaction illustrates why evaluating transmission investment independently of renewable support can be misleading. The cost difference between flat and status-quo subsidies, however, stays almost the same before and after expansion. This is confirmed by almost identical benefit-to-cost ratios of grid expansion in these two scenarios. This follows directly from the finding

in the preceding paragraph that most of the cost difference is driven by factors other than congestion.

In this paper, I exploit multiple useful institutional features present in Germany. The country combines a long history of large-scale wind deployment with a single national wholesale electricity price and a transmission network inherited from an electricity system dominated by coal and nuclear generation. Wind resources are most abundant in the North, while major demand centers lie farther south and west. Planning for the north–south transmission expansion began in the early 2010s, reflecting the policy relevance of adapting this legacy network to a generation mix increasingly concentrated in wind-rich regions. Renewable policy has also responded directly to the geography of wind investment. German regulators have long differentiated wind subsidies according to local wind productivity, awarding higher subsidy rates to turbines at less productive locations. They have also temporarily restricted auction awards in export-constrained northern regions of Germany. These regulations illustrate that the spatial mismatch created by renewable entry has been a concern for policymakers.

The setting is favorable for estimating the wind-entry response to spatial incentives. I observe twenty entry cohorts from 2004 to 2023, covering a long period of large-scale deployment. The Renewable Energy Sources Act (EEG) provides a twenty-year support horizon, allowing me to construct the ex-ante expected lifetime revenues of each project rather than relying on contemporaneous revenues. Lifetime revenues vary substantially across locations and cohorts because wind resources differ, turbine technologies evolve, and support varies by location. This provides rich variation in lifetime revenue allowing me to control for persistent regional differences and common cohort shocks.

Identification of entry responses to lifetime revenue is further aided by the fact that wind projects are largely insulated from the local congestion costs created by their entry. Germany has one national wholesale price, renewable generators have historically been largely compensated when curtailed, and developers do not bear the cost of reinforcing the existing transmission network. These regulations make the interaction between renewable siting and network congestion effectively one-sided. In particular, local congestion does not directly enter the lifetime revenue measure used in the entry model. This reduces an important potential confounding channel: high project revenue is not mechanically a proxy for unobserved favorable local transmission access.

The paper contributes to three strands of literature. First, it relates to renewable siting and locational investment incentives. The value of renewable generation varies with resource quality, displaced generation, and network access (Lin, 2016; Sexton et al., 2021). Lamp and Samano (2023) document spatial misallocation of solar generation in Germany, including the role of transmission constraints. Schmidt and Zinke (2023) and Katzen and Leslie (2024) study distorted siting incentives under uniform or zonal electricity prices; related work examines differentiated support and network charges (Ambec et al., 2026; Grimm et al., 2019; Tangerås and Wolak, 2019; Wagner, 2019). Other studies address policy uncertainty, technological progress, reliability, and intermittent generation (Ambec and Crampes, 2019; Chen, 2025; Covert and Sweeney, 2026; Elliott, 2026). My contribution

is to exploit rich variation from existing spatial subsidies to estimate the response of wind turbine entry to changes in revenue. Rather than imposing a spatial reallocation, this allows me to derive their location choice based on the changed incentives from different spatial subsidies. I further tease apart the effect of nodal pricing on wind turbine entry without changing the full electricity market design.

Second, the paper relates to transmission investment and renewable integration. Transmission affects renewable utilization and market efficiency (De Cannière, 2026; Dorsey-Palmateer, 2020; Fell et al., 2021; Hausman, 2025; LaRiviere and Lyu, 2022). Gonzales et al. (2023) estimate how market integration induces renewable entry, while Doshi (2026) studies wind investment following grid expansion. Arkolakis and Walsh (2023) embed electricity transmission in a spatial model of clean growth, and Johnston et al. (2026) examine interconnection barriers. I study the reverse policy channel: how subsidy-induced wind locations change congestion costs and the value of a grid expansion. Combining estimated entry with endogenous redispatch and curtailment in a network model with loop flows, I quantify when and to what extent locational support complements or substitutes for transmission investment during grid adjustment.

Third, the paper connects to spatial and network economics, where the location of activity and the value of infrastructure depend on network frictions (Allen and Arkolakis, 2014). Fajgelbaum and Schaal (2020) study investment across congested transportation links. In shipping, Brancaccio et al. (2017) show that trade geography and vessel availability determine transport costs, while Brancaccio et al. (2024) show how port investment creates congestion spillovers across the network. Unlike routable shipments, electricity follows physical network constraints. My contribution is to show how changing investment incentives at network nodes alters congestion and the returns to expanding links. The central contribution is therefore to connect private siting incentives to the physical transmission network and to show that the spatial design of renewable support changes not only current congestion costs but also the economic value of subsequent grid expansion.

The remainder of the paper proceeds as follows. Section 2 describes the data. Section 3 presents the institutional setting and constructs expected lifetime wind revenues. Section 4 estimates the onshore wind-entry model. Section 5 introduces the electricity-dispatch and pricing model. Section 6 evaluates the subsidy and transmission counterfactuals, and Section 7 concludes.

2 Data

I collect data on power generation plants in Germany, wind turbine technology, wind speed, subsidies for wind turbines, electricity market outcomes, the physical properties of the electric grid and planned expansion projects.

Power generation plants. I observe the universe of past and present German power generation plants with their exact location. The dataset is publicly available and provided by the German regulator for electricity, gas, telecommunications, railway and post markets (Bundesnetza-

gentur, hereafter BNA). The data set includes the beginning and end date of operation, the installed capacity and energy source. Crucially, for wind turbines I observe the exact model of each installed wind turbine including its height and rotor diameter. Additionally, for each wind turbine the data set features an indicator that allows me to know in which auction they were granted their subsidy. For a subset of all onshore wind turbines it includes the ratio between expected generated electricity of the same turbine model at the actual site and at a reference location defined by the regulator. This is called the quality factor. Its denominator is the reference yield which I also observe separately for the most common wind turbine models provided by FGW (Association for Wind Energy and other Decentralised Energies). These measures are important to calculate the effective subsidy obtained. I complement the information on power generation plants with plant-specific efficiencies, emission factors, fuel and transportation costs which are used to construct marginal costs for 2023. The information is provided through the Merit Order Tool of the Institute of Energy Economics at the University of Cologne (EWI).

Power curves. For most models of the largest wind turbine manufacturers I observe the power curve. The power curve is a function that maps given wind speed in meters per second into electricity produced. I obtain this data from The Wind Power which is a commercial data provider to the industry commonly used by planners when deciding on location and wind turbines for their wind project. With location specific wind speed data the power curve allows to project the expected electricity output at a given location for a specific wind turbine model.

Wind speed. I work with average as well as hourly wind speed data. The former is in meters per second at the height of 100 meters in 250-by-250-meter grid cells. The dataset is freely available, provided by the Global Wind Atlas and based on the ERA5 dataset from the European Centre for Medium-Range Weather Forecasts (ECMWF) for the years 2008 to 2017. The hourly wind data comes from the same source but covers the year 2023 for a 0.25 by 0.25 degree resolution.

Wind turbine subsidies. For the years 2004 up until 2023 I have collected all feed-in tariffs for renewable energy plants as well as the quantity-averaged outcomes of the pay-as-bid auctions that have gradually superseded feed-in tariffs starting 2017. This information comes from the transmission grid operators (TSOs). The subsidy rule is based on exact commissioning date which I have used to match subsidy regimes to individual wind turbine projects.

Electrical grid. Information on all substations in Germany comes from JAO, a service provider for TSOs in Europe. The same is the case for high voltage transmission lines connecting these substations. The dataset also includes important properties of the lines such as their length, resistance and reactance. The grid information is extracted for the beginning of 2024. Information on projected costs, connecting substations and capacities of the newly planned high voltage direct current (HVDC) transmission cables has been collected by hand directly from official documents of the TSOs.

Electricity market outcomes. The TSOs report the monthly average spot market prices for wind energy. This measure is needed to calculate the effective wind turbine subsidy. By TSO I use

hourly data from BNA on realized renewable generation, imports/ exports and electricity demand as well as load from hydro-pumped storage. From ENTSO-E I obtain actual hourly generation along with unavailabilities for all generation units with an installed capacity above 100MW. For the year 2023 I observe curtailment at the TSO-level accessible through the Netztransparenz initiative of the TSOs.

2.1 Wind speed distribution

Germany's geography is such that the North is more favorable for wind turbine deployment. The North of Germany is rather flat and windy as seen in Figure 1. The Middle and South of the country are characterized by low mountain ranges leading to on average lower wind speeds but also to some regional areas of larger wind speed. These areas are generally less accessible, though.

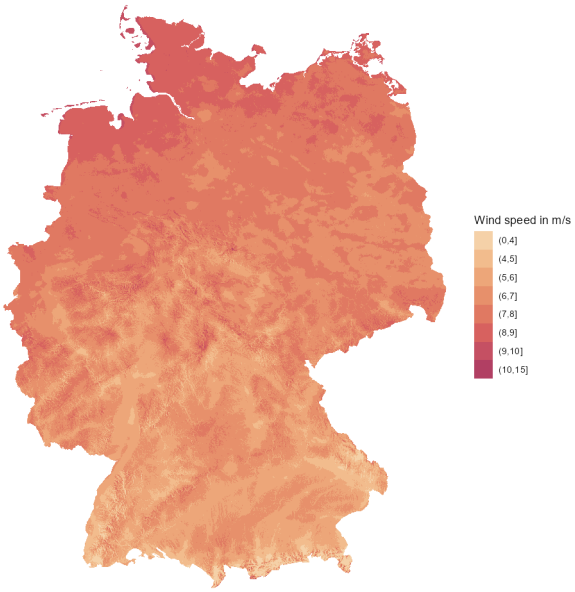
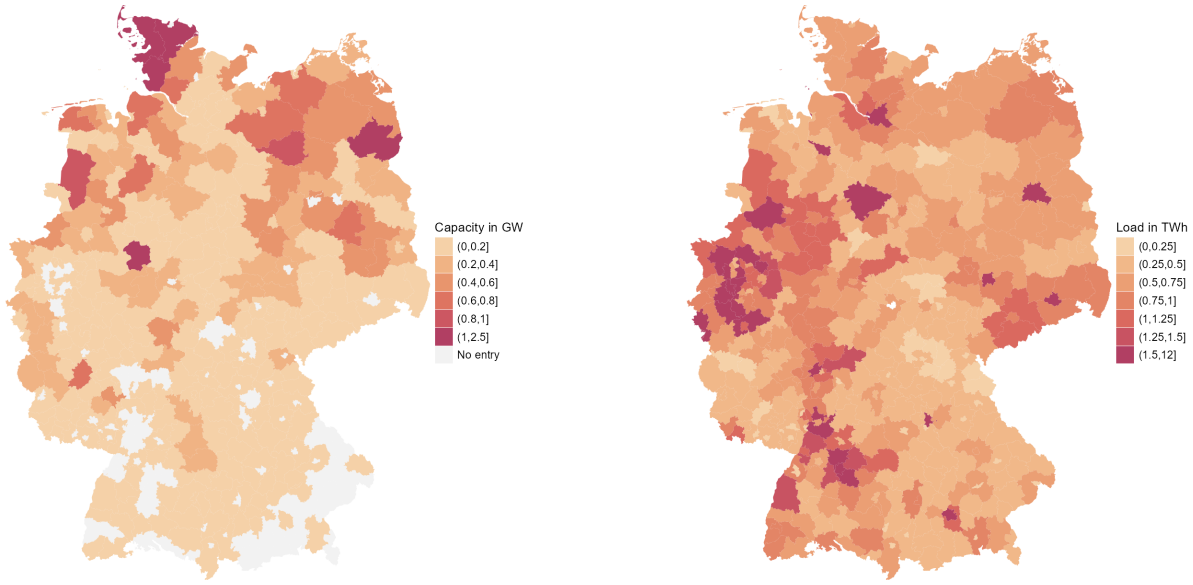


Figure 1. Average onshore wind speed at a height of 100 meters

2.2 Wind turbine locations and load centers

In Figure 2 we can see that wind capacity installed is mainly concentrated in the very North. We can further observe that in the South there are multiple counties entirely unexplored which is also true for the West. This is driven by high population density, inaccessible mountain ranges and regional political resistance. The installed wind capacity correlates strongly with regions of high average wind speeds. The figure further reflects policy decisions that I will detail in the institutional background. The right panel shows that electricity demand is concentrated especially in the West and South West, geographically far from the predominant locations of installed wind capacity in the North.



(a) Cumulative installed onshore wind capacity

(b) Average yearly electricity load

Figure 2. Onshore wind capacity and electricity demand

2.3 Grid congestion

The German electrical grid is historically constructed to connect the coal rich regions of the West and East, as well as nuclear power plants to the large demand centers in the West and South West. It has therefore little capacity to transport electricity from the very North to the rest of Germany. Looking at the cumulative wind generation together with the German coal and nuclear exit exactly this is now needed, though.

Table 1 shows the development of grid congestion together with wind turbine deployment. The German electricity market works in two stages where in a day-ahead market load and renewable generation are projected and the market clears without taking network constraints into account. On the actual day in any given moment demand and supply of electricity have to be exactly equal in Germany (including imports and exports). The regulator therefore adjusts dispatch taking the potentially restricted grid into account. There are two common tools the regulator uses to balance supply and demand under network constraints. First, they can ramp down certain conventional power plants previously dispatched in the day-ahead clearing and ramp up others instead which is defined as redispatch. Alternatively, the operator can ramp down renewable power plants defined as curtailment. This means that they generate more than is actually injected into the system. This effectively creates wasted renewable energy.

Table 1. Evolution of redispatch, curtailment and wind capacity

	Redispatch		**Curtailment**		**Total wind capacity**
	TWh	Mio. Euros	TWh	Mio. Euros	GW
2013	4.4	113	0.5	44	34.2
2017	18.5	392	5.5	610	56.1
2021	20.4	590	5.8	807	63.7

The table shows that both measures scale with the installed wind energy capacity. This is clear when comparing 2013 and 2017. Redispatch increased fourfold while curtailment rose by a factor of 10. At the same time cumulative wind capacity increased by a factor of 1.6. From 2017 to 2020 the regulator restricted wind turbine entry in the very far North which coincided with a comparatively smaller increase in congestion measures comparing 2017 and 2021 even though wind capacity still increased significantly. Redispatch and curtailment increased by 10 and 5 percent, respectively, while cumulative wind capacity changed by 13 percent. This suggests that there is a spatial component to how wind turbine entry affects congestion which is the main focus of this paper. The fact that these measures cost almost EUR 1.4 billion in 2021 further highlights that tackling the congestion issue can lead to a potentially significant relief in cost.

As a response to the poorly suited grid infrastructure for increased wind turbine entry in the far North the regulator has planned three major transmission lines split into five projects. These are planned to be operational from 2026 and 2028 onward. They are shown in Figure 3. We can see that four of them aim to alleviate the described issue connecting the North to demand centers in the West and South West.

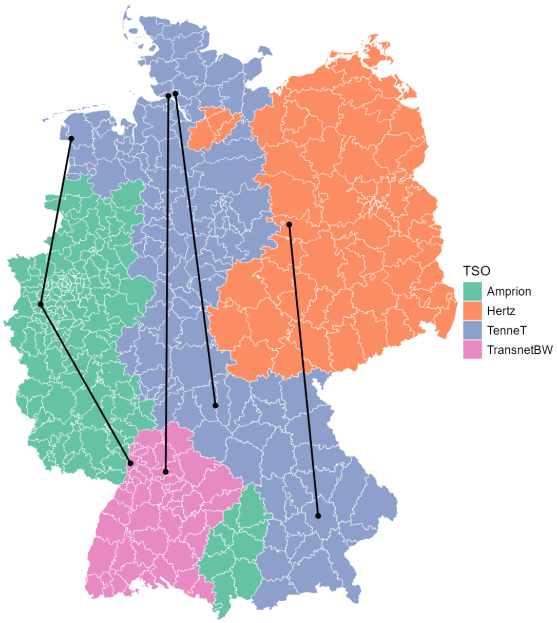


Figure 3. The five planned HVDC transmission lines and the TSOs

3 Institutional Context

Germany has pursued ambitious wind-energy expansion for much of the past two decades, although the extent of this ambition has varied over time. Rapid expansion during the 2000s and early 2010s gave way to a more controlled deployment path in the mid-2010s, in part because of rising congestion-management costs. Since 2021, policy has shifted sharply back toward expansion, with statutory targets requiring around 87 percent more wind capacity by 2030 relative to the level of wind capacity installed at the end of 2025. The long history of deployment is useful for the empirical analysis because I observe twenty entry cohorts between 2004 and 2023, while EEG support is fixed for a twenty-year remuneration horizon. I can therefore measure the ex-ante expected lifetime revenue relevant for entry rather than relying on contemporaneous annual revenues.

In this section I focus on the spatial incentives embedded in the Renewable Energy Sources Act (EEG), in particular the reference yield model, which adjusts support according to local wind conditions. Crucially, it does not reward entry in locations that have a high value for the electricity system. I further detail how this dimension is also missing in other institutional features.

Revenue of wind turbine projects. Wind investment in Germany has been supported through the EEG throughout the period I study. The precise rules changed repeatedly, from administratively set feed-in tariffs to direct marketing and, eventually, auctions. For the analysis, these institutional changes serve one main purpose: they map a project's entry cohort, location and year together with the wind turbine model into its expected lifetime revenue. I implement the applicable rules cohort by cohort and provide the full remuneration schedules in the Appendix 8.2.

To fix notation, let g denote a location and c the year in which a project j enters, which I refer to as its entry cohort. Let $t \in \{1, \dots, 20\}$ denote a calendar year during the project's operating life. The twenty-year horizon corresponds to the common support duration under the EEG. I write q_{jcgt} for expected electricity production in remuneration year t which can be decomposed into the hourly raw wind speed vector $\mathbf{w}_{gt}$ mapped by the power curve $F_j(.)$ of the wind turbine model. We take s_{jcgt} for total remuneration and hence annual revenue is

$$r_{jcgt} = q_{jcgt} s_{jcgt} = F_j(\mathbf{w}_{gt}) s_{jcgt}, \tag{1}$$

and the expected discounted lifetime revenue is

$$V_{jcg} = \sum_t \beta^{t-1} \mathbb{E}[r_{jcgt}] = \sum_t \beta^{t-1} \mathbb{E}[q_{jcgt} s_{jcgt}]. \tag{2}$$

The remuneration term s_{jcgt} accommodates both the earlier feed-in-tariff system and later direct marketing. Under a fixed feed-in tariff, it is simply the applicable statutory payment a_{jcgt}. Under direct marketing, the operator sells its output on the electricity market and receives a market

premium whenever the applicable EEG value exceeds the relevant wind market value. I write

$$s_{jcgt} = p_{jt} + \max\{a_{jcgt} - m_t, 0\}, \tag{3}$$

where m_t is the expected wind market value in remuneration year t and p_{jt} is the electricity price at which the energy is sold. The wind market value is calculated monthly by the TSOs and captures the average electricity price at which wind energy has sold. Total remuneration equals the applicable value plus a spread for profitably selling the electricity, $p_{jt} - m_t$, whenever the market premium is positive. If the market revenue exceeds that value then a project simply gets the electricity price p_{jt}. The auction system introduced an auction into direct marketing. The statutory payment a_{jcgt} is consequently auctioned off instead of fixed by the regulator.

Reference yield model. The central spatial feature of onshore support is the reference yield model, which adjusts remuneration for the quality of the wind site. The reference yield is the electricity that the same turbine type and hub height would produce over five years at a standardized legal reference site. It therefore makes the applicable EEG value a_{jcgt} project and location specific. Let Q^{site}_{jcg} denote expected five-year production at the actual site and Q^{ref}_{jcg} the corresponding reference yield at the legal reference site. I denote the quality factor by

$$\phi_{jcg} = 100 \frac{Q^{\text{site}}_{jcg}}{Q^{\text{ref}}_{jcg}}. \tag{4}$$

A value below 100 therefore describes a site with lower expected production than the reference site. The physical definition of the reference site changed over time, most importantly with the introduction of the auction regime, and I use the definition applicable to each entry cohort.

Before auctions, onshore projects generally received a relatively high initial payment followed by a lower basic payment. The quality factor determined how long the higher payment remained in place: projects at weaker-wind sites retained the initial remuneration for longer. The reference yield model therefore partly compensated locations with lower wind productivity.

The auction regime introduced from 2017 changed both how the level of support is determined and how the reference-yield adjustment operates. Bids are stated for a project at the 100-percent reference site. If z_j denotes the relevant auction value for project j at that reference site, the site-specific applicable value in remuneration cohort c can be written schematically as

$$a_{jcg} = z_j \Gamma_c(\phi_{jcg}), \tag{5}$$

where $\Gamma_c(.)$ denotes the cohort-specific statutory correction schedule. The correction is greater than one at weaker sites and below one at sufficiently strong sites. The auction value is adjusted for site quality and the resulting applicable value governs the constant remuneration over the full support horizon. Thus, the reform can be viewed as a move from adjusting the *duration* of the high tariff to

adjusting the *level* of a single applicable value.

For this paper, the important feature is that this adjustment is limited. The reference yield model makes low-wind locations more attractive than they would be under a geographically uniform payment, but it does not equalize expected revenue across sites. More importantly, the correction is based on wind productivity, not on the value of the resulting electricity to the transmission system. Neither ϕ_{jcg} nor $\Gamma_c(\phi_{jcg})$ directly incorporates local grid congestion, redispatch costs, or the marginal value of an additional MWh of wind energy at location g.

Congestion and private wind revenues. The institutional rules above matter for measuring the expected lifetime revenue V_{jcg}, but they provide no direct congestion signal to wind investors. This distinction is particularly important in Germany because congestion can make an additional MWh of wind substantially less valuable to the electricity system in one part of the grid than in another.

Other elements of market design further insulate private project revenues from local congestion. Germany operates as a single bidding zone, so internal transmission constraints do not translate into locational wholesale prices which could enter through the direct marketing regulation. Power purchase agreements between wind projects and industrial plants are uncommon over the study period. Renewable generation has priority in dispatch, and grid-induced curtailment has historically been largely compensated. Under the historical curtailment rules, plants commissioned from 2012 onward were generally compensated for 95 percent of revenues lost through curtailment; once forgone revenues in a calendar year exceeded one percent of annual revenues, additional curtailment was compensated at 100 percent. The exact compensation mechanism changes over the sample, but the economic point is the same: virtually all of private revenue loss created by network congestion is compensated rather than borne by the wind producer.

Grid-connection rules reinforce this by giving developers a legal right to grid connection. They only bear the cost of connecting a project to the legally determined connection point, whereas the costs of optimizing, reinforcing, and expanding the existing network are borne by the network operator. Wind developers therefore do not face the full network cost generated by their location choice.

Together, these rules imply that spatial differences in expected revenue V_{jcg} arise through wind productivity and the design of EEG remuneration and not through a direct price for local transmission congestion. The temporary grid expansion area (NAG) between 2017 and 2020 is an important exception: it restricted annual auction awards in congested northern regions to 58 percent of average entry over 2013–2015, but did so through a coarse quantity restriction rather than a continuous congestion price. The outlined institutional framework is useful empirically because project revenues vary substantially across space while local congestion itself is largely excluded from private wind revenues.

4 Wind Turbine Entry

I model onshore wind deployment as the outcome of competitive entry by wind developers. The purpose of the model is to recover the intensive-margin response of local wind investment to changes in expected lifetime revenue. It allows me to map a specific subsidy regime s into a spatial allocation of wind turbines. Consistent with the notation introduced in Section 3, let g index locations and c index entry cohorts, where $c \in \{2004, \ldots, 2023\}$.

Descriptive entry patterns. Table 2 summarizes onshore entry over the sample period.[1] Conditional on positive entry, the average onshore county–cohort cell receives about 20 MW of new capacity and has expected discounted lifetime revenue of approximately EUR 3 million per MW. Onshore entry is sparse: among the roughly 6,000 county–cohort cells, there are about 2,500 positive-entry observations. Of the 400 German counties 99 do not see any wind turbine entry. Among these 85 are urban counties according to the Federal Institute for Research on Building, Urban Affairs and Spatial Development (BBSR). The remaining counties are almost exclusively in the state of Bavaria which is known for its strict rules on wind turbine entry. Rather than imposing a common model on both the extensive and intensive margins, I condition the estimation on county–cohort cells with positive observed entry. The model therefore asks how much capacity enters once a location is active, not whether a previously inactive location becomes available for wind development. Most of these counties have high population density or politically unfavorable conditions and it is therefore unlikely that a counterfactual under the same budget constraint would lead to sudden exploration of these areas. The positive entry counties are spread all over the country such that the assumption does not limit spatial reallocation at the level of spatial granularity used in my counterfactuals. The institutional framework further shields entry from local congestion, as explained above, such that the fact that a county has zero entry does not correlate with local congestion.

Table 2. Summary statistics for onshore wind turbine entry

Average entry (MW)	Average lifetime revenue (EUR/MW)	Positive entry	Zero entry
19.46	3,168,846	2,587	3,433

Entry model. For each turbine model j entering location g in cohort c, Section 3 defines expected discounted lifetime revenue V_{jcg}. I aggregate these project-level values to the county–cohort level and treat the resulting capacity-weighted average as the value of a MW of entry in that cell.

[1] Offshore wind is not part of the entry model estimated. There are very few cohorts in which there is entry making estimation challenging. Current policy based on the reference yield model focuses on onshore wind turbines which is what I aim to change in counterfactuals. Substitution between onshore and offshore projects is unlikely to be a large factor given that project scope and complexity are very different.

The entry model therefore assumes homogeneous entry within a county–cohort cell but explicitly captures technological differences across cohorts and counties.

Let $\mathcal{J}_{cg}$ denote the set of turbines entering in (c, g) and let K_j denote turbine j's capacity in MW. Aggregate entry is

$$k_{cg} = \sum_{j \in \mathcal{J}_{cg}} K_j, \tag{6}$$

and expected lifetime revenue per MW is

$$v_{cg} = \frac{\sum_{j \in \mathcal{J}_{cg}} V_{jcg}}{k_{cg}}. \tag{7}$$

Differences in turbine models, hub heights, local wind conditions, and the applicable remuneration rules enter through the project-level values constructed in the preceding section before being aggregated into the county-cohort revenue. This creates substantial variation in lifetime revenue across both space and cohorts. Importantly, as described in Section 3 this variation is driven by wind productivity, technology, and the legal subsidy regime and not by local congestion itself.

I assume competitive entry by atomistic developers with rational expectations. Within a county–cohort cell, developers are homogeneous in the entry model and earn the same expected lifetime revenue per MW v_{cg}. They take expected remuneration and prevailing local input prices as given. Development requires locally scarce inputs such as suitable land, grid-connection opportunities, permitting capacity, and other development services. As aggregate entry increases, competition for these inputs raises their equilibrium price and hence the common development cost per MW faced by developers. I summarize this relationship in the per MW cost function

$$c_{cg}(k_{cg}) = F_{cg} + \alpha k_{cg}, \qquad \alpha > 0, \tag{8}$$

where F_{cg} captures the fixed entry cost. Free entry implies the following condition

$$v_{cg} = F_{cg} + \alpha k_{cg}, \qquad k_{cg} > 0. \tag{9}$$

Identification and estimation. I invert (9) to relate entry to lifetime revenue and bring the following model to the data

$$k_{cg} = \mu_g + \delta_c + \lambda_1 v_{cg} + \lambda_2 NAG_{cg} + \varepsilon_{cg}, \qquad k_{cg} > 0. \tag{10}$$

The fixed effect μ_g captures persistent regional differences in development costs, while δ_c absorbs nationwide changes in turbine investment costs, financing conditions, permitting, and other common determinants of entry costs. Together with the variable NAG_{cg}, they capture the fixed entry cost. I control for the grid expansion area (NAG), which restricted auction awards in designated northern counties between 2017 and 2020. The control interacts NAG county membership with the national share of capacity in each cohort originating from auction awards made during the restriction period.

This accounts for the delay between auction awards and commissioning and captures the differential exposure of NAG counties to a direct restriction on entry. All active developers face the same equilibrium cost per MW, which rises with aggregate entry because local development inputs are scarce. The parameter λ_1 measures the intensive-margin response of entry to a change in expected lifetime value per MW. I collect remaining variation in ε_{cg}.

The German institutional setting removes an important potential confounder from this relationship. Because wind producers face a national wholesale price, are largely compensated for curtailment, and do not pay for reinforcement of the existing transmission network, expected revenues are not mechanically a proxy for unobserved grid access quality.

Nevertheless, other sources of endogeneity remain. The revenue measure is constructed from projects that were actually developed, including their precise sites and technologies. Developers select these characteristics partly in response to unobserved local development conditions, such as land availability, connection costs, and permitting requirements. The remaining cost shocks in ε_{cg} can therefore influence both installed capacity and the observed revenue per MW. In that case, an OLS regression of entry on revenue would not recover the intensive-margin response to an exogenous change in project value.

I address this problem by instrumenting observed lifetime revenue with *potential revenue*, providing identification under assumptions on the timing of project development and the realization of shocks. I assume that developers, conditional on having decided to enter, choose county and cohort based on potential revenue using regional wind conditions and the prevailing subsidy framework before choosing exact sites and turbine technologies. More detailed information about site-specific development costs and constraints becomes available as projects are developed and these choices are made. I assume that these unanticipated development-cost shocks are orthogonal to the earlier revenue opportunities, conditional on state and cohort fixed effects and the NAG control.

To construct potential revenue, I hold turbine technology and potential locations fixed rather than using the technologies and exact sites of realized entrants. I use an Enercon E70/2300 turbine at a hub height of 100 meters and average expected generation across all grid cells in each county. I combine this generation with the applicable EEG remuneration rules in each cohort to calculate discounted lifetime revenue per MW. For the pre-auction regimes, I apply the cohort-specific fixed tariff. For auction-supported projects, I use the official national bid ceiling for the relevant auction rounds in place of realized auction outcomes. Auction outcomes show that awards are typically close to the auction ceiling announced far earlier. The auction ceiling is therefore a good indicator for potential support. Where cohorts contain different remuneration regimes, I combine the corresponding components using their observed capacity shares. For all regimes, I adjust the subsidy based on the reference yield model. Thus, the instrument captures the revenue potential associated with wind resources and policy rules, rather than the particular technologies and sites eventually selected within a county.

I estimate equation (10) on the 2,587 onshore county–cohort observations with positive entry.

Table 3 reports OLS and IV estimates using the same sample, NAG control, and state and cohort fixed effects. Column (2) is my preferred IV specification, with

$$\widehat{\lambda}_1 = 13.805. \tag{11}$$

Expected lifetime revenue is measured in millions of 2023 euros per MW, so an increase of EUR 1,000,000 in lifetime revenue per MW corresponds to approximately 13.8 MW of additional local entry. This corresponds to two to three average-sized onshore wind turbines. Evaluated at the sample means, the estimated intensive-margin entry elasticity is 2.82. The first-stage coefficient on potential revenue is 0.746 and the heteroskedasticity-robust first-stage F-statistic is 198.73.

Table 3. Onshore entry model: OLS and instrumental variables

Dependent Variable:	Entry	
Model:	(1)	(2)
	OLS	IV
Panel A: Entry equation		
Lifetime revenue per MW	3.669***	13.805***
	(0.637)	(2.190)
NAG exposure	-8.537*	-3.034
	(4.881)	(4.776)
Panel B: First stage		
Potential revenue		0.746***
		(0.053)
NAG exposure		-0.465***
		(0.078)
F-statistic		198.73
State fixed effects	Yes	Yes
Cohort fixed effects	Yes	Yes
Observations	2,587	2,587

Notes: The sample contains onshore county–cohort observations with positive entry. Panel A reports new entry in MW on expected discounted lifetime revenue per MW, expressed in million 2023 euros, and the NAG exposure control. Column (1) estimates the preferred specification by OLS. Column (2) instruments expected lifetime revenue with the potential revenue instrument. Panel B reports the corresponding first stage. All specifications include state and cohort fixed effects. Standard errors in parentheses are heteroskedasticity-robust. Significance: *** 1%, ** 5%, * 10%.

The IV estimate exceeds the corresponding OLS coefficient of 3.669, suggesting that the OLS association understates the response of local capacity to expected revenue. The preferred estimate uses variation in project value after accounting for persistent differences between states, common cohort-level changes, and the direct entry restriction captured by NAG exposure. Because estimation is conditional on positive-entry county–cohort cells, I interpret the coefficient as an intensive-margin response relevant for reallocating wind investment across active locations, rather than an effect on

whether a previously inactive county receives its first project.

The crucial feature of the model for the rest of the paper is that it allows me to map expected lifetime revenue v_{cg}^s under a spatial design of wind support s into a spatial allocation of wind turbines k_{cg}^s. Keeping the local cost schedule fixed, the entry condition relative to a change in revenue is

$$k_{cg}^s = \max\left\{0,\ k_{cg} + \widehat{\lambda}_1 \left(v_{cg}^s - v_{cg}\right)\right\}. \tag{12}$$

5 Electricity Dispatch

The dispatch model maps a spatial allocation of wind capacity based on subsidy design s, k_{cg}^s, into hourly wind generation and then into electricity-market outcomes. The German electricity market works in two stages. Electricity is first traded in a single national bidding zone without internal transmission constraints. After market clearing, transmission-system operators adjust generation when the resulting injections are incompatible with the physical grid. I mirror this sequence. In Stage 1, conventional generation together with gross renewable generation is dispatched nationally according to the merit order meaning that generation plants are dispatched according to increasing marginal cost. The wholesale price is set as the marginal cost of the marginal plant. In Stage 2, generation is redispatched and renewables are curtailed across the four German transmission-system-operator (TSO) areas—50Hertz, TenneT, Amprion, and TransnetBW—subject to the transmission network. I allow for transmission constraints across but not within TSOs. The county assignment to each TSO is shown in Figure 3. More than 90 percent of renewable curtailment concerns wind energy over the sample period. I therefore model wind curtailment alone which is only allowed for when redispatch cannot produce a feasible allocation. In my model changing the location of wind can leave nationwide generation almost unchanged while substantially changing the amount of redispatch and curtailment required to operate the grid. This is an important feature for the counterfactuals.

The dispatch model evaluates each wind allocation in the same 2023 electricity-system environment. Demand, net imports, non-wind renewable generation, storage operation, the conventional generation fleet, marginal generation costs, and the transmission network are held fixed across subsidy regimes. Offshore wind is also held fixed. The only object that changes with subsidy design is the spatial allocation of onshore wind turbines implied by the entry model. I therefore interpret differences across scenarios as the short-run system consequences of reallocating onshore wind capacity, rather than as a forecast of a new general equilibrium in the electricity market.

Representative hours and electricity supply. Let $r \in \mathcal{R}$ index the four TSO areas and $h \in \mathcal{H}$ index hours. I select 1,000 representative 2023 hours using k-medoids clustering. The clustering uses, for each TSO, pre-wind residual demand and gross wind generation, giving eight system-state variables in total. Unlike k-means clustering, medoids are actual hours rather than

synthetic averages, each selected observation preserves the joint realization of demand, wind, and other system conditions. I detail the precise implementation of the clustering in Appendix 8.3. Let n_h denote the number of 2023 hours represented by medoid h, so that $\sum_h n_h = 8{,}760$.

Let D_{rh} denote observed domestic electricity load augmented by pumped-storage charging. Let $\widetilde{D}_{rh}$ be domestic load minus exogenous net imports. Net imports are fixed because the object of interest is congestion within Germany rather than endogenous adjustment at international interconnectors. Let R_{rh} collect all fixed renewable generation other than wind, including solar, biomass, hydro, other renewables, and observed pumped-storage generation. Storage charging and generation are held at their observed 2023 levels rather than optimized intertemporally.

Let $i \in \mathcal{I}_r$ index conventional generating units in TSO r. Unit i has marginal cost m_i and available hour-specific dispatch capacity $\overline{G}_{ih}$. Marginal cost combines fuel and transport costs, plant efficiency, carbon costs, and variable operating costs,

$$m_i = \frac{f_i + \tau_i}{\eta_i} + p^{CO_2}\frac{e_i}{\eta_i} + u_i. \tag{13}$$

Here, f_i is the fuel price per MWh of thermal input, τ_i is the corresponding fuel-transport cost, η_i is plant efficiency, p^{CO_2} is the EU ETS allowance price per tonne of CO_2, e_i is the fuel-specific emissions factor per MWh of thermal input, and u_i is the non-fuel variable operating cost per MWh of electricity. Hence m_i is measured in EUR/MWh of electricity. I assume competitive cost-based dispatch and abstract from strategic bidding and market power. I add reserve generation capacity to the observed power plants in each TSO. I assume it to have the same marginal cost as the observed power plant with the highest marginal cost. This ensures that the technology is only employed as a last resort to establish feasibility of serving demand. I report the actual usage of this technology throughout.

I account for conventional-plant availability using realized hourly outage patterns observed for generation units with more than 100 MW capacity. To all other plants I assign each energy source a fixed average unavailability rate and apply the same rate to all plants using that source. Available capacity is therefore time variant for some but not all plants and remains identical across subsidy scenarios. Generation satisfies

$$0 \le G_{ih} \le \overline{G}_{ih}. \tag{14}$$

Each representative hour is solved independently. I therefore abstract from start-up costs, minimum-run constraints, ramping, and intertemporal storage arbitrage. These restrictions matter for a detailed reconstruction of unit commitment, but are less central for relative congestion consequences of changing the geographic distribution of wind while holding the rest of the electricity system fixed.

Hourly wind production. The entry model changes wind capacity at the county–cohort level, while dispatch requires hourly generation. I construct a common hourly productivity profile

for each active county–cohort cell and hold it fixed across policy scenarios. Continuing the notation from the entry model, let g denote a county, c an entry cohort, and $\mathcal{J}_{cg}$ the set of observed turbines in that cell. For turbine j, I evaluate realized 2023 wind conditions at its location and scale wind to turbine hub height. A direct mapping of raw reanalysis wind speeds through turbine power curves tends to overpredict realized wind generation, a well-known issue in wind-generation simulation (Geiger et al., 2026; Gruber et al., 2019). I therefore apply a multiplicative wind-speed correction, calibrated by TSO and technology against hourly 2023 observed generation plus curtailment, before mapping wind speed through the turbine-specific power curve. The details are in Appendix 8.1. Let q_{jh} denote the resulting gross output in hour h and K_j the turbine's installed capacity. The county–cohort capacity factor is

$$CF_{cgh} = \frac{\sum_{j \in \mathcal{J}_{cg}} q_{jh}}{\sum_{j \in \mathcal{J}_{cg}} K_j}. \tag{15}$$

The wind data used here is realized hourly 2023 ERA5 weather rather than the long-run-normalized wind distribution used to form expected lifetime revenues. For the 2023 cohort, output is set to zero in hours preceding each turbine's observed commissioning date, preserving the within-year commissioning pattern.

Let k^s_{cg} denote installed onshore capacity under subsidy regime s. Gross onshore wind in TSO r is then

$$W^{s,\text{on}}_{rh} = \sum_{g:r(g)=r} \sum_{c} CF_{cgh} k^s_{cg}, \tag{16}$$

and total gross wind generation is

$$W^s_{rh} = W^{s,\text{on}}_{rh} + W^{\text{off}}_{rh}, \tag{17}$$

where offshore generation is common across scenarios. Hence a subsidy counterfactual scales the amount of onshore capacity in existing county–cohort cells while holding fixed their observed site and technology composition and their hourly wind productivity. Historical curtailment is not added to W^s_{rh}; it is used only to reconstruct gross historical wind when selecting and validating the representative hours. Curtailment is determined endogenously in the dispatch model below.

Stage 1: national market dispatch. Stage 1 represents market clearing in Germany's single bidding zone. Internal transmission constraints are ignored and zero marginal cost generation, such as wind as well as other renewable generation, enters ahead of conventional generation. The national residual requirement for conventional generation is

$$Q^s_h = \sum_r \left(\widetilde{D}_{rh} - R_{rh} - W^s_{rh} \right). \tag{18}$$

If $Q_h^s > 0$, conventional units are dispatched in increasing order of m_i according to

$$\begin{aligned} \min_{\{G_{ih}\}} \quad & \sum_i m_i G_{ih} \\ \text{s.t.} \quad & \sum_i G_{ih} = Q_h^s, \\ & 0 \leq G_{ih} \leq \overline{G}_{ih}. \end{aligned} \tag{19}$$

Let $G_{ih}^{1,s}$ be the solution of the above problem under subsidy regime s. If gross fixed generation exceeds national demand, conventional generation is set to zero and the excess is removed in the subsequent minimum-curtailment step. Let $G_{rh}^{1,s} = \sum_{i \in \mathcal{I}_r} G_{ih}^{1,s}$ denote Stage 1 conventional generation in TSO r and

$$C_h^{1,s} = \sum_i m_i G_{ih}^{1,s} \tag{20}$$

denote minimal generation cost without grid constraints.

The single national wholesale electricity price in Germany is derived from the first stage problem as the Lagrangian multiplier on the national balance constraint, $\sum_i G_{ih} = Q_h^s$. This is equivalent to the change in minimal generation cost from an additional MWh demand anywhere in Germany and therefore does not capture local scarcity of electricity which can vary depending on network constraints.

Stage 2: market balance under network constraints. Stage 2 asks how closely the market allocation can be implemented on the physical transmission network. The four TSO areas are the network nodes. I retain physical transmission lines that connect different TSOs and abstract from bottlenecks within a TSO. Let κ_{rh} denote wind curtailment. Net injection into the transmission network at a specific TSO is

$$I_{rh}^s = G_{rh} + R_{rh} + W_{rh}^s - \kappa_{rh} - \widetilde{D}_{rh}. \tag{21}$$

I use a linear real-power representation of the grid which I detail in Appendix 8.4. The mapping H translates TSO injections into physical cross-TSO line flows where flow on line ℓ is

$$Z_{\ell h}^s = \sum_r H_{\ell r} I_{rh}^s, \qquad -\overline{Z}_\ell \leq Z_{\ell h}^s \leq \overline{Z}_\ell. \tag{22}$$

Electricity on alternating current lines flows according to physical laws captured by H. It cannot be actively directed but can mainly be affected by changing nodal injections. The individual line capacity limit $\overline{Z}_\ell$ is also derived from physical properties and the feature that captures network constraints. Capacity limits are negative and positive but symmetric depending simply on the geographic direction in which electricity flows. I treat the grid as a four-node transmission system with observed cross-TSO transfer constraints. I abstract from within-TSO congestion, reactive

power, and voltage constraints. In this model national balance of supply and demand is captured by

$$\sum_r I^s_{rh} = 0. \tag{23}$$

I do not add a separate endogenous electrical loss function. The observed total-load measure already includes transmission and distribution losses, so the realized 2023 loss component is embedded in D_{rh}. Because observed demand is held fixed across subsidy scenarios, these losses are held fixed as well. The linear transmission model itself is lossless, however, so the counterfactuals abstract from changes in electrical losses that would result from changing the geographic pattern of power flows.

Renewable priority over conventional generation is represented by making wind curtailment a last-resort feasibility instrument. Before final redispatch, I find the smallest aggregate amount of wind that permits a feasible network allocation,

$$\min_{\{\kappa_{rh}\},\{G_{rh}\}} \sum_r \kappa_{rh}, \qquad 0 \le \kappa_{rh} \le W^s_{rh}, \tag{24}$$

subject to conventional capacity limits $\overline{G}_{ih}$, the nodal injections in (21), the line constraints in (22) and national balance in (23). Among allocations requiring the same minimum curtailment, I select the one requiring the least redispatch. Curtailment compensation does not enter this optimization: wind is curtailed only to restore physical feasibility, not because curtailment is cheaper than conventional redispatch.

Given the resulting κ^s_{rh}, the final Stage 2 allocation minimizes the absolute TSO-level deviation from the Stage 1 market outcome,

$$\min_{\{G_{rh}\}} \sum_r \left| G_{rh} - G^{1,s}_{rh} \right|, \tag{25}$$

subject to the same generation, balance, and transmission constraints imposing minimal curtailment $\kappa_{rh} = \kappa^s_{rh}$. The objective reflects the institutional sequence in which the national market clears first and the system operator subsequently changes that market schedule only as much as necessary to operate the network. Conditional on the required generation in each TSO, conventional units within the TSO are still dispatched according to ascending marginal cost.

Let $G^{2,s}_{ih}$ denote the resulting TSO-level dispatch. Generation cost with the grid constraints is

$$C^{2,s}_h = \sum_i m_i G^{2,s}_{ih}. \tag{26}$$

I measure one-sided redispatch volume as

$$RD^s_h = \frac{1}{2} \sum_r \left| G^{2,s}_{rh} - G^{1,s}_{rh} \right|, \tag{27}$$

and redispatch cost as the change in conventional generation cost,

$$RC_h^s = C_h^{2,s} - C_h^{1,s}. \tag{28}$$

Finally, I attach an ex-post compensation measure to curtailed wind. Let $\bar{s}_{rh}^s$ denote the average remuneration of supported wind generation in TSO r and hour h under subsidy regime s. Curtailment cost is

$$CC_h^s = \sum_r \bar{s}_{rh}^s \kappa_{rh}^s, \tag{29}$$

and total system cost reported in the results is

$$TC_h^s = C_h^{2,s} + CC_h^s. \tag{30}$$

I also report the sum of redispatch and curtailment cost $RC_h^s + CC_h^s$ to isolate the congestion-management cost relative to the unconstrained national market outcome.

Locational marginal prices. The German electricity market wholesale price is derived from the stage 1 problem therefore assuming that there is no varying scarcity of electricity by TSO which is equivalent to saying that the least-cost dispatch solution is always feasible without ever leading to binding network constraints. In order to capture local scarcity in the electricity price we need to set up an alternative dispatch model. It consists of the objective of stage 1 subject to the full network constraints of stage 2. The problem asks what the minimal generation cost is under network constraints. This problem is solved in markets that follow nodal pricing meaning that the electricity supplied and demanded in a specific geographic area served by a specific node has a different price than at other nodes. Here, this translates into four distinct prices per hour which is one price per TSO. I do not change the design of the German electricity market but derive these resulting so-called locational marginal prices (LMPs) only to use them as a local scarcity signal for the counterfactual congestion-adjusted subsidy. It is supposed to induce wind turbine entrants to internalize the system effect of their location choice.

The network-constrained pricing problem minimizes the generation cost $\sum_i m_i G_{ih}$ subject to conventional capacity limits $\overline{G}_{ih}$, the nodal injections in (21), the line constraints in (22) and national balance in (23).

Let ν_{rh}^s, μ_h^s, $\eta_{\ell h}^{+,s}$ and $\eta_{\ell h}^{-,s}$ be the multipliers of the resulting Lagrangian

$$\begin{aligned}\mathcal{L}_h^s = &\sum_i m_i G_{ih} + \sum_r \nu_{rh}^s \left(\widetilde{D}_{rh} - G_{rh} - R_{rh} - W_{rh}^s + \kappa_{rh} + I_{rh}^s\right) - \mu_h^s \sum_r I_{rh} \\ &+ \sum_\ell \eta_{\ell h}^{+,s} \left(\sum_r H_{\ell r} I_{rh}^s - \overline{Z}_\ell\right) + \sum_\ell \eta_{\ell h}^{-,s} \left(-\sum_r H_{\ell r} I_{rh}^s - \overline{Z}_\ell\right) + \mathcal{B}_h^s,\end{aligned} \tag{31}$$

where $\mathcal{B}_h^s$ collects the generation- and curtailment-bound terms. In order to capture local scarcity we ask how the minimal generation cost changes with an additional MWh demand in TSO r. This

is the definition of the LMPs. Due to the envelope theorem this is captured by the derivative of the Lagrangian with respect to $\widetilde{D}_{rh}$

$$p^s_{rh} \equiv \left.\frac{\partial \mathcal{L}^s_h}{\partial \widetilde{D}_{rh}}\right|_* = \nu^s_{rh}, \tag{32}$$

which can be rewritten as

$$p^s_{rh} = \mu^s_h - \sum_\ell H_{\ell r}\left(\eta^{+,s}_{\ell h} - \eta^{-,s}_{\ell h}\right) \tag{33}$$

where μ^s_h is the national scarcity component and the rest is the local congestion component. When no transmission line constraint binds, $\eta^{+,s}_{\ell h} = \eta^{-,s}_{\ell h} = 0$ for all ℓ and all TSO prices coincide.

A simple measure of the strength of spatial congestion in hour h is the LMP range

$$\Delta p^s_h = \max_r p^s_{rh} - \min_r p^s_{rh}. \tag{34}$$

These locational prices later provide the congestion signal used in the congestion-adjusted subsidy counterfactual.

Aggregation and simulation. For any hourly outcome x_h, I report the represented-hour-weighted average

$$\overline{x} = \sum_{h\in\mathcal{H}} \omega_h x_h, \qquad \omega_h = \frac{n_h}{8{,}760}. \tag{35}$$

Annual quantities can equivalently be recovered as $\sum_h n_h x_h$. The same representative hours and weights are used for every subsidy regime, so comparisons do not reflect changes in the distribution of weather or demand.

The annual validation in Table 4 shows that hourly clustering does a good job at matching the observed gross wind generation, curtailment as well as redispatch. The dispatch model does not match the observed 2023 levels of redispatch and wind curtailment closely but performs well matching the sum of them. This is consistent with the four-node representation resulting in the omission of within-TSO bottlenecks and modeling curtailment as only chosen for feasibility. I therefore use the dispatch model primarily for internally consistent comparisons across alternative wind allocations evaluated in the same electricity-system environment.

Table 4. Validation of status-quo electricity-market outcomes against observed 2023 outcomes

Outcome	Actual full 2023 (TWh)	Actual, weighted medoids (TWh)	Status-quo model (TWh)
Gross wind generation	149.53	149.42	147.27
Wind curtailment	7.23	7.00	3.00
One-sided redispatch	10.07	9.64	15.61

Notes: Actual full 2023 uses all observed hours. Actual, weighted medoids evaluates the same observed series at the 1,000 representative hours and weights each medoid by the number of hours assigned to it. Status-quo model values are annualized using the same representative-hour weights. Gross wind equals observed wind injection plus observed curtailment. Observed one-sided redispatch equals one half of total upward plus downward redispatch MWh.

Table 5 reports selected model-implied outcomes for the observed wind allocation before introducing the policy counterfactuals. Transmission constraints increase average conventional generation cost from EUR 2.108 million to EUR 2.174 million per hour and require 1.78 GWh of one-sided redispatch. Average gross wind production is 16.8 GWh per hour, of which 0.34 GWh is curtailed. The reserve needs to be used in 3.6 percent of the hours while its average contribution is low. The corresponding locational marginal prices are substantially lower in 50Hertz and TenneT than in Amprion and TransnetBW, with an average within-hour spread of EUR 39/MWh. This indicates that the former are often export-constrained as they cover the windy northern regions while the latter are commonly import-constrained covering the demand centers in the west and southwest. The large spread further demonstrates that there is substantial congestion between TSOs making electricity supply substantially more valuable in some regions than in others. These spatial price differences motivate the congestion-adjusted subsidy detailed in the next section.

Table 5. Status-quo electricity-market outcomes, 2023

Outcome	Status quo
Dispatch	
Generation cost w/o grid constraint (EUR/h)	2,108,608
Generation cost w/ grid constraint (EUR/h)	2,174,184
Redispatch volume, one-sided (MWh)	1,781.7
Redispatch cost (EUR/h)	65,577
Gross wind generation (MWh)	16,812.2
Wind generation used (MWh)	16,469.5
Wind curtailment (MWh)	342.7
Curtailment cost (EUR/h)	30,817
Redispatch + curtailment cost (EUR/h)	96,394
Total cost (EUR/h)	2,205,001
Reserve	
Hours with reserve use (percent)	3.6
Reserve generation (MWh/h)	18.8
Prices	
National one-zone price (EUR/MWh)	107.23
50Hertz LMP (EUR/MWh)	96.92
TenneT LMP (EUR/MWh)	98.02
Amprion LMP (EUR/MWh)	112.02
TransnetBW LMP (EUR/MWh)	135.69
Within-hour LMP range (EUR/MWh)	39.13

Notes: Dispatch, cost, curtailment, wind, and price outcomes are represented-hour-weighted averages over the 1,000 representative hours, representing 8,760 actual hours in 2023. Total cost equals constrained Stage 2 conventional generation cost plus ex-post wind-curtailment compensation. Reserve-use statistics are calculated over the status quo scenario's solved representative hours, weighted by represented hours; reserve generation includes zero-use hours. The national one-zone price is obtained from the Stage 1 unconstrained least-cost pricing problem; TSO LMPs are from the network-constrained least-cost pricing problem. The within-hour range is the represented-hour-weighted mean of the difference between the maximum and minimum TSO LMP in each hour.

6 Counterfactuals

I use the estimated entry response and dispatch model to compare three spatial designs of onshore wind support. The first is the observed status quo described in Section 3, under which the reference yield model adjusts support for local wind productivity but does not price transmission congestion. The second removes this spatial adjustment and makes the supported rate geographically flat within each entry cohort thereby mimicking free entry with a guaranteed support level. The third instead adjusts the supported rate using lagged locational marginal prices, thereby exposing entry to the marginal value of electricity at different locations in the transmission system. In both counterfactuals, offshore wind is unchanged and the government's lifetime onshore subsidy budget is held fixed cohort by cohort. The counterfactual subsidy is applied to all entry cohorts in the sample period 2004 to 2023.

6.1 Counterfactual subsidy design

Let B_c^{SQ} denote the undiscounted lifetime government expenditure on onshore wind support implied by the status-quo subsidy regime in cohort c. Let b_{cg}^s denote the corresponding undiscounted lifetime government payment per MW in county g under counterfactual subsidy regime s. Both counterfactuals satisfy

$$\sum_g k_{cg}^s b_{cg}^s = B_c^{SQ} \qquad \text{for every cohort } c. \tag{36}$$

Importantly, this is a budget constraint rather than a capacity constraint. The amount of entry can change because a different spatial allocation of the same support budget changes expected lifetime project values and hence entry through equation (12).

Geographically flat support. For the flat counterfactual, I choose one supported rate a_c^F for each entry cohort and apply it to every active onshore county. A project under fixed remuneration receives a_c^F per MWh. A directly marketed project continues to sell electricity in the market and receives a premium only when a_c^F exceeds the expected wind market value. Thus the counterfactual removes the location-specific reference-yield adjustment but does not otherwise turn directly marketed projects into fixed-price projects.

For a candidate a_c^F, I construct the implied lifetime revenue v_{cg}^F using the same expected generation per MW and the same mix of remuneration types as in the observed county–cohort cell. Equation (12) then gives k_{cg}^F. I choose a_c^F so that the resulting government payments satisfy the government budget constraint in equation (36). Because the supported rate affects both subsidy payments per MW and the amount of entry receiving them, the budget condition determines the flat rate jointly with counterfactual entry.

Relative to the status quo, the flat policy removes the partial compensation that the reference yield model provides to weaker-wind sites and the lower support provided to stronger-wind sites. The

payment rate itself no longer depends on local wind conditions, although expected project value still does because a MW installed at a windier site produces more electricity. The flat policy therefore rewards wind productivity more directly, but it remains silent about whether that production is located on the valuable or congested side of the transmission network.

Congestion-adjusted support. This counterfactual replaces the current wind-productivity-based spatial adjustment with a congestion signal. I start from the observed cumulative capacity of onshore wind turbines in 2004. I derive the LMPs and national wholesale price for 2004 and use them to define the congestion signal for the 2005 entry cohort. Exposing entrants in 2005 to the congestion signal leads to counterfactual entry in that year which I use to derive a new congestion signal for 2006 entrants. I continue iteratively until the end of the sample period. This is done based on demand, imports/ exports, other renewables and the grid of the year 2023. The congestion signal uses an approximation to past LMPs and is defined as

$$\rho_{r,c-1} = \frac{\overline{p}_{r,c-1}}{\overline{p}^0_{c-1}}, \tag{37}$$

where

$$\overline{p}_{r,c-1} = \frac{\sum_{h \in \mathcal{H}} n_h W^{LMP}_{rh,c-1} p^{LMP}_{rh,c-1}}{\sum_{h \in \mathcal{H}} n_h W^{LMP}_{rh,c-1}}.$$

The price $\overline{p}_{r,c-1}$ is the wind-generation-weighted average LMP in TSO r and $\overline{p}^0_{c-1}$ is the average national price based on stage 1 of the dispatch model. The wind-generation weights are important as wind generation in the same area is highly correlated over time and is often largest in hours where the LMPs are at their extremes. The hourly wind weighting allows me to capture this without deviating from annual to hourly subsidies. The supported rate offered to cohort c is

$$a^{LMP}_{rc} = \alpha_c \rho_{r,c-1}. \tag{38}$$

The same fixed-remuneration and direct-marketing rules used in the flat counterfactual then map a^{LMP}_{rc} into lifetime revenue v^{LMP}_{cg} and government subsidy payments. The common component α_c is chosen so that lifetime government expenditure again satisfies the budget constraint in equation (36).

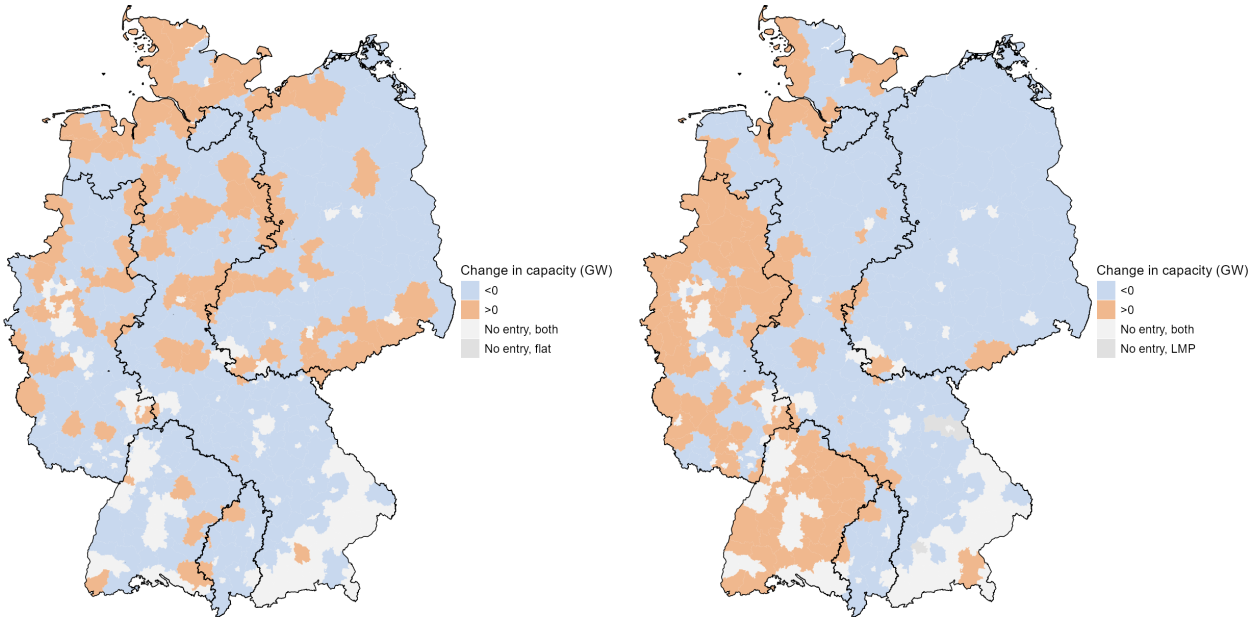
The policy depends on the *relative* local value of electricity rather than the overall electricity price level. A TSO with an LMP below the national price receives a multiplier below one, while a TSO in which an additional MWh is relatively valuable receives a multiplier above one. Because the dispatch model has four TSO nodes, the congestion adjustment is common to counties within a TSO; county-level entry nevertheless remains heterogeneous because wind productivity and wind turbine model mix differ across counties.

The economic contrast across the three regimes is sharp. Status-quo support differentiates locations according to wind productivity, flat support does not differentiate the supported rate

geographically at all, and LMP-adjusted support differentiates locations according to their marginal value to the transmission system.

6.2 Spatial reallocation of wind entry

Figure 4 shows the resulting change in total onshore capacity by county, summing entry over the 2004–2023 cohorts. The maps report counterfactual capacity minus status-quo capacity, such that blue counties lose entry and orange counties gain entry from switching to the counterfactual subsidy. Counties in light gray have no entry in both scenarios while darker gray indicates counties without entry under the counterfactual policy only.



(a) Flat minus status quo subsidy **(b)** LMP minus status quo subsidy

Figure 4. Change in onshore wind capacity under alternative subsidy designs

The flat policy removes any spatial signal. It therefore does not reward weak wind locations with higher support as under the status quo. The common payment shifts investment toward locations where a MW capacity produces more electricity. The most-productive counties in the far north therefore see more entry but so do locations in the low mountain ranges in the middle of the country. Table 6 summarizes the capacity installed by TSO and subsidy regime. This is the capacity fed into the electricity dispatch model after turning it into wind generation. The flat subsidy further pushes wind entry into TenneT, which covers the windy northwest, relative to the status quo while reducing entry in all other TSOs.

The LMP-adjusted policy replaces the penalty based on wind productivity by a penalty based on local congestion. Wind-abundant parts of northern Germany are export-constrained leading to low locational marginal prices, reducing support there. Higher locational prices in import-constrained

southern and western parts of Germany make entry more attractive there. Relative to the flat policy, the resulting reallocation is directed away from the low-price northern regions and toward counties in the southwest and west located within the TransnetBW and Amprion TSOs. At the same time, some of the strongest wind-resource locations in the north continue to gain capacity relative to the status quo: high physical productivity can compensate for lower support. The map therefore illustrates the trade-off the LMP rule is designed to capture. Efficient siting need not mean moving all wind south; it means balancing the productivity of a site against the system value of the electricity produced there. Overall, total capacity is slightly lower under the two counterfactual subsidy regimes.

Table 6. Total onshore wind capacity by TSO and support scheme

	Capacity (GW)		
TSO	SQ	Flat	LMP
50Hertz	15.86	15.57	14.51
Amprion	11.47	11.25	11.79
TenneT	21.36	21.53	20.78
TransnetBW	1.66	1.55	2.89
Total	50.34	49.90	49.97

Notes: Capacity is summed over the 2004–2023 onshore entry cohorts. Offshore wind is excluded. SQ denotes the status quo; Flat denotes geographically flat support; LMP denotes congestion-adjusted support.

6.3 Planned transmission expansion

The spatial subsidy counterfactual changes where generation is built. A second policy instrument is to change the grid itself. I therefore add the major north–south HVDC projects currently planned or under construction: A-Nord, Ultranet, SuedLink Vorhaben 3, and SuedOstLink Vorhaben 5. Each project contributes 2 GW of controllable transfer capacity resulting in 8 GW of additional inter-TSO capacity in the four-node model. A-Nord connects TenneT to Amprion, Ultranet connects Amprion to TransnetBW, SuedLink Vorhaben 3 connects TenneT to TransnetBW, and SuedOstLink Vorhaben 5 connects 50Hertz to TenneT. At the level of aggregation used here, SuedLink Vorhaben 4 is not separately represented because both of its endpoints lie within TenneT.

I model these projects as additional lossless controllable transfers between their endpoint TSOs and solve the same 2023 dispatch problem again. These lines increase the ability to move electricity from wind-rich northern and eastern regions toward western and southern demand centers, thereby potentially relieving bottlenecks and reducing redispatch and renewable curtailment.

The grid exercise is deliberately ex post with respect to wind entry. I first determine the wind allocation under each subsidy regime on the existing grid and then operate that same allocation with

the planned grid. Hence the comparison isolates the operational value of transmission expansion conditional on where subsidy policy has caused wind to locate. It does not allow developers to anticipate the new lines and change entry in response. This distinction is useful for showing the interaction between the two policy instruments. Spatially targeted support and transmission expansion can both reduce the same congestion externality, so a subsidy that already steers entry toward high-value locations can reduce the marginal value of additional grid capacity. Conversely, a subsidy that directs more wind toward congested locations can make grid expansion substantially more valuable.

6.4 Electricity-market effects

I next evaluate the six combinations of subsidy regime and grid expansion using the dispatch model in Section 5. All reported operating outcomes are evaluated on the same 1,000 representative hours, representing all 8,760 hours of 2023. Table 7 reports the main dispatch outcomes.

Table 7. Electricity-market outcomes across subsidy regimes, with and without the planned lossless HVDC grid, 2023

Outcome	SQ	Flat	LMP	SQ+Grid	Flat+Grid	LMP+Grid
Generation cost w/o grid (EUR/h)	2,108,608	2,118,285	2,120,076	2,108,608	2,118,285	2,120,076
Generation cost w/ grid (EUR/h)	2,174,184	2,185,270	2,165,479	2,121,204	2,131,273	2,127,902
Redispatch volume, one-sided (MWh)	1,781.7	1,803.3	1,539.1	662.8	671.6	510.8
Redispatch cost (EUR/h)	65,577	66,985	45,403	12,597	12,989	7,826
Gross wind generation (MWh)	16,812.2	16,716.7	16,690.3	16,812.2	16,716.7	16,690.3
Wind generation used (MWh)	16,469.5	16,376.0	16,455.9	16,704.9	16,612.7	16,615.9
Wind curtailment volume (MWh)	342.7	340.6	234.4	107.3	104.0	74.4
Curtailment compensation (EUR/h)	30,817	30,470	20,562	9,594	9,248	6,489
Redispatch + curtailment cost (EUR/h)	96,394	97,455	65,965	22,191	22,237	14,316
Total cost (EUR/h)	2,205,001	2,215,740	2,186,041	2,130,799	2,140,522	2,134,392
Hours with reserve use (percent)	3.6	3.7	2.4	0.0	0.0	0.0
Reserve generation (MWh/h)	18.8	20.0	9.7	0.0	0.0	0.0

Notes: Cost, redispatch, curtailment, and wind outcomes are represented-hour-weighted averages over the identical set of 1,000 representative hours, representing 8,760 actual 2023 hours. Reserve statistics use each scenario's solved representative hours with represented-hour weights. Reserve generation is averaged across all solved hours, including zeros. SQ denotes the status-quo subsidy regime, Flat the geographically flat subsidy counterfactual, and LMP the congestion-adjusted subsidy counterfactual. +Grid denotes operation of the corresponding wind-entry allocation with the planned HVDC grid expansion. Total cost equals constrained Stage-2 generation cost plus curtailment compensation.

Column one simply reproduces the outcomes from Table 5. Column two shows that relative to the status quo, the flat subsidy produces less gross wind generation and increases unconstrained generation cost by EUR 10,000 per hour. This is driven by the fact that overall capacity is lower under the flat subsidy. When entry is pushed to relatively more productive sites, this increases subsidy payments per MW of capacity and as we operate under the same budget constraint less capacity can be supported with the same budget. Here, the effect of less capacity outweighs the

positive effect of moving to more productive sites. This explains why before imposing network constraints the status quo subsidy does a better job. Including network constraints confirms this ranking. Redispatch is slightly higher such that the generation costs with grid constraints are EUR 11,000 higher than under the status quo. Total curtailment is similar such that total cost increases by 0.5 percent relative to the status quo. The total cost increase per hour due to congestion is EUR 1,000 which amounts to only ten percent of the total cost increase. This finding reveals a limitation of the current spatial subsidy design: at the four-TSO level, its wind-productivity adjustment provides little congestion relief relative to free entry under a common support level. Annually, the total cost increase is EUR 94 million which is equivalent to 7 percent of the EUR 1.4 billion spent on onshore wind turbine support in 2023. The policy change has negligible effects on the frequency and extent of reserve capacity usage.

The congestion-adjusted policy also leads to lower gross wind production than under the status quo, such that unconstrained generation cost increases, but the spatial reallocation simultaneously reduces congestion. Redispatch falls to 1.54 GWh per hour, curtailment falls to 234 MWh per hour, and redispatch plus curtailment cost falls to EUR 66,000 per hour. Total modeled electricity-system cost is EUR 19,000 per hour below the status quo. This translates into a reduction of about 0.9 percent or EUR 166 million annually which is 12 percent of onshore wind turbine support in 2023. Wind actually used stays almost the same such that the effect comes from making a larger share of wind generation usable by the grid. This is also reflected in the share of hours needing reserve capacity dropping by one percentage point. Without transmission expansion, the congestion-adjusted support outperforms both status quo and flat subsidy.

Adding the planned HVDC projects reduces congestion under every subsidy regime. Under the status quo, one-sided redispatch falls from 1.78 to 0.66 GWh per hour, curtailment from 343 to 107 MWh per hour and reserve capacity usage is entirely absent. The cost difference between flat and status-quo support remains almost unchanged once the planned grid is added: total modeled electricity-system cost is EUR 2.141 million per hour under Flat+Grid and EUR 2.131 million under SQ+Grid. This confirms that status quo and flat subsidy design lead to similar patterns and levels of congestion. The lowest total operating cost among the six scenarios is now achieved by combining the status quo support with the planned grid. The congestion-adjusted subsidy proves remarkably competitive on its own, though. Without any grid expansion, the congestion-adjusted subsidy achieves roughly 26 percent of the cost reduction obtained by combining the status quo with the costly planned grid investment. These results show that the incremental value of grid expansion depends on the spatial incentives embedded in the subsidy.

I show a cost-benefit analysis of the grid expansion under the three different subsidies in Table 8. I define the hourly benefit of the grid as the reduction in total modeled electricity-system cost when the same wind allocation is operated with the planned HVDC links. For comparison with this flow benefit, I annualize the EUR 14.0 billion projected gross investment cost of the four modeled inter-TSO projects over 40 years at a one-percent annual discount rate. This gives an annualized

cost of EUR 426.4 million, or EUR 48,673 per hour. Operating and maintenance costs are not included.

Table 8. Hourly benefit and annualized capital cost of the planned HVDC grid across wind-subsidy regimes, 2023

Wind policy	Grid benefit (EUR/h)	Grid capital cost (EUR/h)	Benefit-cost ratio
SQ	74,203	48,673	1.52
Flat	75,218	48,673	1.55
LMP	51,650	48,673	1.06

Notes: The hourly grid benefit equals total modeled electricity-system cost without the planned HVDC grid minus total modeled electricity-system cost with the planned HVDC grid for the same wind-subsidy regime. Total system cost is constrained Stage-2 generation cost plus curtailment compensation. Benefits are calculated on the identical six-scenario representative-hour sample used in Table 7. Grid capital cost annualizes the summed gross cost of the active inter-TSO projects, equal to EUR 14.0 billion, over 40 years at an annual discount rate of one percent, giving EUR 426.4 million per year or EUR 48,673 per hour. The benefit-cost ratio is hourly benefit divided by hourly annualized grid capital cost.

The marginal value of the grid is largest under flat support: its operating benefit is about EUR 75,000 per hour, fifty percent higher than the annualized capital cost under the maintained assumptions. Under the status quo the cost-benefit ratio is very similar in line with the results above. Under congestion-adjusted support the benefit-cost ratio falls to a level just above one, so the same expansion is only just cost-covering because part of the congestion problem has already been addressed by changing where wind enters. The cost-benefit analysis confirms that transmission expansion and congestion-adjusted subsidies show a significant degree of substitutability. Evaluating either policy in isolation can therefore be misleading when the regulator controls both the incentives governing renewable siting and the capacity of the network connecting those sites to demand.

Table 9 shows the same mechanism through prices. The national one-zone price changes across subsidy regimes because their wind allocations produce different amounts of electricity, but it is unchanged when only the grid is expanded because stage 1 does not include transmission constraints. The LMPs instead respond strongly to both policy instruments.

Under the flat subsidy, the average within-hour LMP range rises very little from EUR 39.13/MWh to EUR 40.43/MWh. The congestion-adjusted policy instead reduces the range to EUR 28/MWh: northern prices rise and the highest southern prices fall. This is direct evidence that the entry response to the congestion signal reduces the spatial mismatch that generated the signal in the first place. The planned grid has an even larger equalizing effect. The LMP range falls to EUR 4.86/MWh under the status quo and EUR 5.03/MWh under flat support. Congestion-adjusted support retains its congestion advantage by leading to a range of EUR 3.03/MWh once the new transfer capacity is available.

The cost measures in this section are electricity-system operating costs from the perspective of the regulator rather than a welfare measure. They include conventional generation costs and the ex-post measure of curtailment compensation, while the subsidy budget is held fixed by construction.

Table 9. Average national and locational electricity prices across subsidy regimes, with and without the planned lossless HVDC grid, 2023

Price measure (EUR/MWh)	SQ	Flat	LMP	SQ+Grid	Flat+Grid	LMP+Grid
National one-zone price	107.23	107.51	107.53	107.23	107.51	107.53
50Hertz LMP	96.92	97.00	99.41	104.11	104.20	105.63
TenneT LMP	98.02	98.05	100.21	104.48	104.55	105.90
Amprion LMP	112.02	112.16	111.69	108.98	109.23	108.66
TransnetBW LMP	135.69	137.07	126.97	108.92	109.19	108.62
Within-hour LMP range (max-min)	39.13	40.43	28.00	4.86	5.03	3.03

Notes: Entries are represented-hour-weighted averages over the same 1,000 representative hours as Table 7. The final row is the represented-hour-weighted mean of the within-hour maximum minus minimum TSO LMP.

They do not include changes in wind-development costs, consumer surplus, or other external benefits of renewable generation. The counterfactuals are therefore best interpreted as quantifying how alternative spatial subsidy rules and grid expansion change the cost of integrating a given renewable transition into the electricity system.

7 Conclusion

This paper studies the spatial allocation of wind investment and transmission capacity as a joint policy problem where grid expansion arrives with a delay. In Germany, the reference yield model affects where wind enters by adjusting support to local wind conditions, while developers are largely insulated from the congestion costs created by their location choice. Transmission expansion then responds to the resulting geography of generation. I combine an estimated wind-entry model with an electricity-dispatch model under grid constraints and endogenous congestion management to evaluate these two policy margins jointly, holding the government subsidy budget fixed.

I show that subsidy design and grid expansion cannot be evaluated independently. Under the observed wind allocation and 2023 market conditions, the planned grid expansion is valuable with a benefit-to-cost ratio of 1.5 in the model, suggesting that the current transmission expansion is closely matched to the expected congestion generated under the status-quo subsidy system ex-post. This remains very similar under the geographically flat subsidy demonstrating that the current subsidy design leads to very similar patterns and level of congestion as a free-entry benchmark under a national wholesale price with a guaranteed support level.

Switching to congestion-adjusted subsidies has a strong effect, though. By reallocating the same subsidy budget toward locations where electricity has greater marginal system value, they reduce redispatch, curtailment and total modeled electricity-system cost without changing the physical grid or abandoning Germany's national bidding zone. On their own, they achieve 26 percent of the cost relief from the grid expansion under the status quo. They also reduce spatial price divergence

substantially. Because part of the congestion problem has already been addressed through better siting, the planned grid expansion is only just cost-covering. Congestion-adjusted support and transmission expansion are therefore imperfect substitutes: one changes where generation is built, while the other changes how easily electricity can be moved after those investments have been made.

The results highlight that the spatial allocation of renewable support is an important policy margin in its own right. This matters particularly in Germany where policymakers plan a large expansion of wind capacity by 2030. Better locational incentives today can reduce the congestion created by future renewable investment and, in turn, the amount of costly transmission expansion required to integrate it.

References

Allen, T. and C. Arkolakis (2014). Trade and the topography of the spatial economy. *The Quarterly Journal of Economics 129*(3), 1085–1140.

Ambec, S. and C. Crampes (2019). Decarbonizing electricity generation with intermittent sources of energy. *Journal of the Association of Environmental and Resource Economists 6*(6), 1105–1134.

Ambec, S., C. Crampes, and S. Lamp (2026). Pricing intermittent renewable energy. TSE Working Paper 1653, Toulouse School of Economics. October 2026.

Arkolakis, C. and C. Walsh (2023). Clean growth. NBER Working Paper 31615, National Bureau of Economic Research.

Bohn, R. E., M. C. Caramanis, and F. C. Schweppe (1984). Optimal pricing in electrical networks over space and time. *The RAND Journal of Economics 15*(3), 360–376.

Brancaccio, G., M. Kalouptsidi, and T. Papageorgiou (2017). Geography, search frictions and endogenous trade costs. NBER Working Paper 23581, National Bureau of Economic Research. Revised October 2018.

Brancaccio, G., M. Kalouptsidi, and T. Papageorgiou (2024). Investment in infrastructure and trade: The case of ports. NBER Working Paper 32503, National Bureau of Economic Research.

Chen, L. (2025). The dynamic efficiency of policy uncertainty: Evidence from the wind industry. Technical report, Working Paper. Revise and Resubmit at Econometrica.

Covert, T. R. and R. L. Sweeney (2026). Winds of change: Technical progress and learning in wind power. Technical report, Working Paper.

De Cannière, C. (2026). Market integration and market efficiency: Evidence from transmission constraints in the belgian electricity sector. Working paper, Toulouse School of Economics. July 2026.

Dorsey-Palmateer, R. (2020). Transmission costs and the value of wind generation for the crez project. *Energy Policy 138*, 111248.

Doshi, G. (2026). Chicken and egg: Electricity transmission and investment in renewable energy. *Journal of Public Economics 256*, 105598.

Elliott, J. T. (2026). Investment, emissions, and reliability in electricity markets. *American Economic Review*. Forthcoming.

European Court of Auditors (2025). Making the eu electricity grid fit for net-zero emissions. Technical Report Review 01/2025, European Court of Auditors.

European Union Agency for the Cooperation of Energy Regulators (2024). Capacities for cross-zonal electricity trade and congestion management. Market monitoring report, ACER.

Fajgelbaum, P. D. and E. Schaal (2020). Optimal transport networks in spatial equilibrium. *Econometrica 88*(4), 1411–1452.

Fell, H., D. T. Kaffine, and K. Novan (2021). Emissions, transmission, and the environmental value of renewable energy. *American Economic Journal: Economic Policy 13*(2), 241–272.

Geiger, D., C. Zink, F. Bär, M. Pfennig, D. Callies, C. Pape, J. Drücke, and L. Pauscher (2026). Assessing the performance of reanalysis and meso-scale model datasets for onshore wind power modelling in germany. *Advances in Science and Research 22*, 131–148.

Gonzales, L. E., K. Ito, and M. Reguant (2023). The investment effects of market integration: Evidence from renewable energy expansion in chile. *Econometrica 91*(5), 1659–1693.

Grimm, V., B. Rückel, C. Sölch, and G. Zöttl (2019). Regionally differentiated network fees to affect incentives for generation investment. *Energy 177*, 487–502.

Gruber, K., C. Klöckl, P. Regner, J. Baumgartner, and J. Schmidt (2019). Assessing the global wind atlas and local measurements for bias correction of wind power generation simulated from merra-2 in brazil. *Energy 189*, 116212.

Hausman, C. (2025). Power flows: Transmission lines, allocative efficiency, and corporate profits. *American Economic Review 115*(8), 2574–2615.

Johnston, S., Y. Liu, and C. Yang (2026). An empirical analysis of the interconnection queue. NBER Working Paper 31946, National Bureau of Economic Research. Reject and Resubmit at Econometrica; revised 2026.

Katzen, M. and G. W. Leslie (2024). Siting and operating incentives in electrical networks: A study of mispricing in zonal markets. *International Journal of Industrial Organization 94*, 103069.

Lamp, S. and M. Samano (2023). (mis) allocation of renewable energy sources. *Journal of the Association of Environmental and Resource Economists 10*(1), 195–229.

LaRiviere, J. and X. Lyu (2022). Transmission constraints, intermittent renewables and welfare. *Journal of Environmental Economics and Management 112*, 102618.

Lin, Y. (2016). Where does the wind blow? green preferences and spatial misallocation in renewable energy sector. CEP Discussion Paper 1424, Centre for Economic Performance, London School of Economics and Political Science.

Saint-Drenan, Y.-M., R. Besseau, M. Jansen, I. Staffell, A. Troccoli, L. Dubus, J. Schmidt, K. Gruber, S. G. Simões, and S. Heier (2020). A parametric model for wind turbine power curves incorporating environmental conditions. *Renewable Energy 157*, 754–768.

Schmidt, L. and J. Zinke (2023). One price fits all? on inefficient siting incentives for wind power expansion in germany under uniform pricing. *The Energy Journal 44*(4), 21–52.

Sexton, S., A. J. Kirkpatrick, R. I. Harris, and N. Z. Muller (2021). Heterogeneous solar capacity benefits, appropriability, and the costs of suboptimal siting. *Journal of the Association of Environmental and Resource Economists 8*(6), 1209–1244.

Tangerås, T. and F. Wolak (2019). Locational marginal network tariffs for intermittent renewable generation. *Available at SSRN 3495488*.

Wagner, J. (2019). Grid investment and support schemes for renewable electricity generation. *The Energy Journal 40*(2), 195–220.

8 Appendix

8.1 Wind Technology and Production

The analysis uses three distinct wind-production objects. First, the statutory reference yield and site-quality factor are legal inputs to EEG remuneration. Second, the entry model requires expected physical generation over a representative operating year. Third, the dispatch model requires hourly generation in the realized 2023 weather environment. The legal object is completed from the reference-yield information described below. The two physical-generation objects instead use hourly ERA5 wind and are kept conceptually separate from the statutory reference-yield calculation.

8.1.1 Imputation of missing turbine power curves

The Marktstammdatenregister reports rated capacity, rotor diameter, and hub height but not turbine power curves. I therefore match the turbine registry to a model-specific power-curve library. Observed manufacturer–model curves are retained whenever available. Historical manufacturer labels that refer to the same turbine technology within the same corporate holding are reconciled before any imputation.

For turbine model j, let K_j denote rated capacity, D_j rotor diameter, and

$$SP_j = \frac{K_j}{\pi(D_j/2)^2} \tag{39}$$

denote specific power. If model j has no observed curve, I first search among observed curves from the same manufacturer and use another manufacturer in the same corporate holding only if no same-manufacturer donor is available. Among admissible donors, rotor diameter is the primary matching characteristic. I retain donor models d whose rotor diameter lies within two meters of the best available rotor match and then choose the donor minimizing

$$\left|\log\left(\frac{SP_d}{SP_j}\right)\right|. \tag{40}$$

The donor pool is fixed before imputation, so an imputed curve never becomes a donor for another turbine.

I convert the donor curve to a capacity-factor curve $CF_d(w)$ and rescale wind speed using the cubic relationship between swept area and wind power. The scaling factor is

$$\zeta_{jd} = \left(\frac{SP_d}{SP_j}\right)^{1/3}, \tag{41}$$

so that the target curve in the partial-load region is

$$\widehat{CF}_j(w) = CF_d(\zeta_{jd} w). \tag{42}$$

A lower-specific-power turbine therefore reaches a given capacity factor at a lower wind speed. The donor's empirical rated and cut-out behavior is retained, capacity factors are restricted to $[0, 1]$, and the final curve is normalized to peak at the target turbine's rated capacity. This procedure is close in spirit to the specific-power rescaling used by Geiger et al. (2026). It preserves observed model curves whenever possible while avoiding a single generic fleet curve; remaining differences in control strategy and environmental conditions are a limitation of the imputation (Saint-Drenan et al., 2020).

8.1.2 Legal reference yield and site-quality completion

For onshore turbines, the EEG quality factor ϕ_{jcg} defined in Equation (4) requires expected production at the actual site relative to production at the statutory reference site. Observed registry and statutory values are retained whenever available. The following procedure is used only to complete missing legal reference-yield and site-quality objects; it is not the physical generation series used for lifetime revenue or dispatch.

Let $\bar{w}^{GWA}_{jg,100}$ denote the Global Wind Atlas long-run mean wind speed at the location of turbine model j in county g. For projects governed by the pre-2017 reference-site definition, I map the 100-meter wind speed to hub height H_j with the logarithmic profile

$$\bar{w}^{GWA}_{jg,H} = \bar{w}^{GWA}_{jg,100} \frac{\log(H_j/0.1)}{\log(100/0.1)}, \tag{43}$$

while the corresponding statutory reference-site wind speed is

$$\bar{w}^{ref}_{j,H} = 5.5 \frac{\log(H_j/0.1)}{\log(30/0.1)}. \tag{44}$$

For the post-2017 auction reference site, the analogous quantities use a power-law profile with exponent 0.25 and a statutory mean of 6.45 m/s at 100 meters,

$$\bar{w}^{GWA}_{jg,H} = \bar{w}^{GWA}_{jg,100} \left(\frac{H_j}{100}\right)^{0.25}, \qquad \bar{w}^{ref}_{j,H} = 6.45 \left(\frac{H_j}{100}\right)^{0.25}. \tag{45}$$

The statutory reference-site wind speed is never adjusted to fit the data.

Because a mean wind speed alone does not determine expected turbine output, I approximate the within-location wind-speed distribution by a Rayleigh distribution when constructing this legal object. If $F_j(w)$ is the turbine power curve introduced in Section 3 and w is Rayleigh distributed with mean μ, expected power is

$$\bar{F}_j(\mu) = \int_0^\infty F_j(w) f_R(w; \mu)\, dw. \tag{46}$$

This is evaluated numerically on a fine wind-speed grid. The simulated five-year reference yield is

$$\widehat{Q}^{\mathrm{ref}}_{jcg} = 5 \times 8760 \times \bar{F}_j(\bar{w}^{ref}_{j,H}). \tag{47}$$

For turbines with both a reported quality factor ϕ^{obs}_{jcg} and an official turbine-specific reference yield $Q^{\mathrm{ref},obs}_{jcg}$, the implied mean site output provides a calibration target. I use a turbine for calibration only when the simulated reference yield is reasonably close to the official value,

$$0.8 \leq \frac{\widehat{Q}^{\mathrm{ref}}_{jcg}}{Q^{\mathrm{ref},obs}_{jcg}} \leq 1.2. \tag{48}$$

For each retained turbine I choose a multiplicative adjustment ϑ_{jcg} to the GWA site wind speed such that the Rayleigh-integrated power curve matches the site yield implied by $\frac{\phi^{obs}_{jcg}}{100} Q^{\mathrm{ref},obs}_{jcg}$. The search is restricted to $\vartheta_{jcg} \in [0.40, 1.25]$; boundary solutions are excluded from the spatial calibration sample.

The turbine-level corrections are noisy and multiple turbines in one wind park should not receive mechanical independent weight. I therefore winsorize the corrections at the first and ninety-ninth percentiles and collapse them to 0.01-degree spatial cells using the median. For target location g, I use the twenty nearest calibration cells with Gaussian weights

$$w_m(g) = \exp\left[-\frac{1}{2}\left(\frac{d_m(g)}{h(g)}\right)^2\right], \qquad h(g) = \max\{10, d_{20}(g)\}, \tag{49}$$

where distances are in kilometers. The weighted local estimate is shrunk toward the national median correction when nearby information is sparse or distant. Reported registry values remain unchanged; the smoothed prediction fills only missing quality factors or reference yields. The resulting correction is best interpreted as an effective site-yield correction rather than pure meteorological measurement error because it can also absorb micrositing, wake, availability, electrical, and other losses embedded in the EEG site-yield concept. Bias correction of gridded wind products using local information is common in wind-power simulation (Gruber et al., 2019).

8.1.3 Hourly ERA5 correction and physical generation

Physical generation for revenue and dispatch is constructed from hourly ERA5 wind. Raw reanalysis wind passed through turbine-specific power curves systematically differs from observed aggregate generation, so I estimate a multiplicative wind-speed correction separately for onshore and offshore wind. For onshore wind I estimate one correction factor for each of the four TSO regions. Offshore wind is grouped into the North Sea fleet connected to TenneT and the Baltic Sea fleet connected to 50Hertz, yielding two offshore correction factors. Let w_{jh} denote ERA5 wind at turbine j mapped to its hub height and let $W^{target}_{\tau rh}$ denote observed gross wind generation for technology group τ and

region r. For candidate factor γ, simulated aggregate generation is

$$W^{sim}_{\tau rh}(\gamma) = \sum_{j \in \mathcal{J}_{\tau r}} F_j(\gamma w_{jh}), \tag{50}$$

and I choose

$$\widehat{\gamma}_{\tau r} = \arg \min_{\gamma \in [0.5, 1.5]} \frac{1}{H} \sum_h \left[W^{sim}_{\tau rh}(\gamma) - W^{target}_{\tau rh} \right]^2. \tag{51}$$

The numerical tolerance is 10^{-4} and the fit is to hourly 2023 generation rather than annual totals.

The observed target is reconstructed gross generation. I start from hourly TSO-level observed onshore and offshore wind generation and add back renewable curtailment in the same TSO and hour. Because the curtailment data identify renewable curtailment but do not separately report its onshore and offshore components, I allocate curtailment using fixed technology shares. In 50Hertz and TenneT, 41 percent of renewable curtailment is assigned to onshore wind and 59 percent to offshore wind. In Amprion and TransnetBW, where no offshore fleet enters the calibration, 100 percent is assigned to onshore wind. Thus

$$W^{target,on}_{rh} = W^{obs,on}_{rh} + s^{on}_r \kappa^{hist}_{rh}, \qquad W^{target,off}_{rh} = W^{obs,off}_{rh} + s^{off}_r \kappa^{hist}_{rh}, \tag{52}$$

with $(s^{on}_r, s^{off}_r) = (0.41, 0.59)$ for 50Hertz and TenneT and $(1, 0)$ for Amprion and TransnetBW. The resulting factors therefore reconcile simulated ERA5 production with estimated gross production before curtailment. They should be interpreted as effective production corrections and are distinct from the EEG-based site-quality completion above.

Expected annual generation for the entry model is intended to reflect long-run wind conditions rather than an unusually windy or calm realization of 2023. I preserve the hourly shape of the 2023 ERA5 series but normalize its local mean to the 2008–2017 ERA5 climatology. If $\bar{w}^{2023}_j$ and $\bar{w}^{clim}_j$ denote the corresponding local means, the normalized series is

$$w^E_{jh} = w^{2023}_{jh} \frac{\bar{w}^{clim}_j}{\bar{w}^{2023}_j}. \tag{53}$$

After mapping this series to hub height and applying $\widehat{\gamma}_{\tau r}$, expected annual generation for a project j in cohort c and location g is

$$q_{jcgt} = 8760 \frac{1}{H} \sum_h F_j\left(\widehat{\gamma}_{\tau(j) r(g)} w^{E,H}_{jh} \right), \qquad t = 1, \ldots, 20. \tag{54}$$

The same expected annual output is used in every year of the twenty-year revenue horizon, abstracting from turbine degradation and secular future changes in wind conditions.

For electricity dispatch, I instead retain the realized hourly 2023 ERA5 field. I map it to hub height, apply the same technology–TSO correction, and evaluate the turbine power curve without the climatological normalization in Equation (53). Thus the revenue calculation uses a long-run-

normalized production profile whereas dispatch holds the realized 2023 weather environment fixed. For turbines commissioned during 2023, output is set to zero before the observed commissioning date.

Table 10. Calibration and validation of wind-speed corrections

Calibration group	Correction factor	Target generation (TWh)	Sim./target before	Sim./target after	Correlation before	Correlation after
Onshore – 50Hertz	0.968	38.87	1.044	0.973	0.979	0.979
Onshore – Amprion	0.886	26.43	1.241	0.959	0.977	0.972
Onshore – TenneT	0.934	52.45	1.129	0.981	0.977	0.975
Onshore – TransnetBW	0.974	3.97	1.028	0.972	0.953	0.950
Offshore – Baltic Sea (50Hertz)	0.913	5.07	1.127	0.990	0.886	0.896
Offshore – North Sea (TenneT)	0.831	22.71	1.390	1.067	0.954	0.928

Notes: The correction factor multiplies ERA5 wind speed before applying the turbine power curve. Target generation is observed 2023 wind injection plus allocated observed curtailment. The onshore correction is calibrated separately for each TSO; offshore correction is calibrated separately for the Baltic Sea/50Hertz and North Sea/TenneT groups. The simulated-to-target ratios compare annual simulated generation with the gross observed target before and after correction. Correlations compare the corresponding hourly generation profiles.

The validation Table 10 reports the six technology–region correction factors together with their hourly fit. The correction factors are below one and successful at reducing the difference to the target generation value overall but at the cost of lower hourly correlation.

8.2 Wind Remuneration and Lifetime Revenue

8.2.1 Onshore remuneration

The onshore revenue construction follows the statutory regime applicable at entry. Before auctions, the commissioning date determines the relevant EEG schedule. Once support is awarded by auction, the auction date also determines the applicable legal regime. The main implementation rules are summarized here; project-specific statutory values are assigned at the finest date frequency required by the law.

For the pre-auction reference-yield model, let ϕ_{jcg} denote the quality factor in percentage points, as in Equation (4). Under the regimes through July 2014, the high initial payment applies for

$$M_{jcg}^{old} = \min\left\{240, 60 + 2\frac{\max\{150 - \phi_{jcg}, 0\}}{0.75}\right\} \tag{55}$$

months. Under the EEG 2014, the corresponding duration is

$$M_{jcg}^{2014} = \min\left\{240, 60 + \frac{\max\{130 - \phi_{jcg}, 0\}}{0.36} + \frac{\max\{100 - \phi_{jcg}, 0\}}{0.48}\right\}. \tag{56}$$

If a tariff transition occurs within a project year, the annual applicable value is the month-weighted average of the two rates. Table 11 reports the ordinary rates used for the 2004–2016 cohorts.

Projects through July 2014 are treated as receiving the applicable fixed feed-in remuneration. From August 2014, direct marketing is used for projects above the statutory feed-in-tariff threshold:

Table 11. Ordinary onshore wind rates before the auction regime

Commissioning period	Regime	Initial value (ct/kWh)	Basic value (ct/kWh)
Jan.–Jul. 2004	earlier 2004 schedule	8.80	5.90
Aug.–Dec. 2004	EEG 2004	8.70	5.50
2005	EEG 2004	8.53	5.39
2006	EEG 2004	8.36	5.28
2007	EEG 2004	8.19	5.17
2008	EEG 2004	8.03	5.07
2009	EEG 2009	9.20	5.02
2010	EEG 2009	9.11	4.97
2011	EEG 2009	9.02	4.92
2012	EEG 2012	8.93	4.87
2013	EEG 2012	8.80	4.80
Jan.–Jul. 2014	EEG 2012	8.66	4.72
Aug.–Dec. 2014	EEG 2014	8.90	4.95
2015	EEG 2014	8.90	4.95
Jan.–Mar. 2016	EEG 2014	8.79	4.89
Apr.–Jun. 2016	EEG 2014	8.69	4.83
Jul.–Sep. 2016	EEG 2014	8.58	4.77
Oct.–Dec. 2016	EEG 2014	8.48	4.72

500 kW during 2014–2015 and 100 kW from 2016. The turbine-level capacity is used for this classification because the data do not fully identify the statutory aggregation of multiple installations.

Projects commissioned in 2017–2018 without an auction identifier and with a pre-auction remuneration assignment are treated as transition projects. They retain Equation (56) and the pre-2017 reference-site definition. The date-specific statutory values used for these projects are shown in Table 12.

Table 12. Statutory values for non-auction EEG 2017 transition projects

Commissioning period	Initial value (ct/kWh)	Basic value (ct/kWh)
Jan.–Feb. 2017	8.38	4.66
Mar. 2017	8.29	4.61
Apr. 2017	8.20	4.56
May 2017	8.12	4.51
Jun. 2017	8.03	4.47
Jul. 2017	7.95	4.42
Aug.–Sep. 2017	7.87	4.37
Oct.–Dec. 2017	7.68	4.27
Jan.–Mar. 2018	7.49	4.17
Apr.–Jun. 2018	7.31	4.07
Jul.–Sep. 2018	7.14	3.97
Oct.–Dec. 2018	6.97	3.87

For auctioned projects, bids are stated for a 100-percent reference site. Let z_j denote the value at that reference site, as in Section 3. When the individual award value is unavailable, I use the capacity-weighted average successful award value of the identified auction round. The site-specific applicable value is

$$a_{jcg} = z_j \Gamma_c(\phi_{jcg}), \tag{57}$$

where the correction schedule Γ_c depends on the statutory regime. Table 13 summarizes the support points. Values between support points are linearly interpolated.

Table 13. Reference-yield correction factors under the auction regimes

Regime / quality factor (%)	50	60	70	80	90	100	110	120	130	140	150
EEG 2017	–	–	1.29	1.16	1.07	1.00	0.94	0.89	0.85	0.81	0.79
EEG 2021	–	1.35	1.29	1.16	1.07	1.00	0.94	0.89	0.85	0.81	0.79
EEG 2023	1.55	1.42	1.29	1.16	1.07	1.00	0.94	0.89	0.85	0.81	0.79

Under the EEG 2017, quality factors below 70 percent use the 70-percent factor; under the EEG 2021, values below 60 percent use the 60-percent factor. Under the EEG 2023, the 50–60

percent portion of the schedule is available only to projects in the "south region"; outside that region values below 60 percent use the 60-percent factor. The EEG 2021 south region rule instead operated through auction allocation and therefore does not change the applicable value conditional on an observed award. The south region includes all of Baden-Württemberg and Saarland as well as virtually all of Bayern and the southern parts of Rheinland-Pfalz and Hessen.

A separate regional intervention applied during the first years of the auction regime through the *Netzausbaugebiet*. From 2017 through 2020, auction awards for onshore wind in a contiguous congested northern area—Schleswig-Holstein, Mecklenburg-Vorpommern, Hamburg, Bremen, and parts of northern Niedersachsen—were subject to an annual quantity cap. The objective was to slow additional wind entry in areas in which existing transmission constraints already caused substantial curtailment and redispatch while north–south grid reinforcement was still under construction. The EEG 2017 set the maximum annual award volume in the area at 58 percent of its average annual gross additions during 2013–2015. Given average additions of about 1,555 MW in those years, the resulting cap was 902 MW per year. The rule restricted where auctioned capacity could enter but did not alter the applicable remuneration of a project conditional on receiving an award; it was abolished with the EEG 2021.

The applicable auction regime is assigned by the auction date rather than the commissioning year alone. In particular, pre-2021 awards remain under the EEG 2017 schedule even if commissioned later; awards from 2021–2022 use the EEG 2021 schedule; and the EEG 2023 schedule applies to 2023 auctions. For the entry calculation, the quality factor is held at its entry-time prediction at the statutory reviews at the beginning of years 6, 11, and 16. This avoids introducing ex-post generation information to ex-ante revenue calculation used in the wind entry decision.

8.2.2 Market-value expectations and lifetime revenue

A directly marketed project sells electricity in the market and receives the EEG premium. The relevant wind market value is a generation-weighted average of wholesale prices during wind-production hours, not the unweighted spot price. For cohort c, I form the entry-time expectation from up to the five preceding annual onshore-wind market values,

$$\bar{m}_c = \frac{1}{|\mathcal{Y}_c|} \sum_{y \in \mathcal{Y}_c} m_y^{obs}, \qquad \mathcal{Y}_c = \{c-1, \ldots, c-5\} \cap \mathcal{Y}^{obs}. \tag{58}$$

When fewer than five preceding observations are available, all available preceding years are used. For projects in cohort c, I set the expected wind market value m_t introduced in Equation (3) equal to $\bar{m}_c$ in every remuneration year t. The resulting expectation is therefore held fixed over the twenty-year project horizon.

For the expected revenue calculation, the expected sales price p_{jt} is also represented by the same

wind market value $\bar{m}_c$. Hence expected total remuneration under direct marketing is

$$s_{jcgt} = \bar{m}_c + \max\{a_{jcgt} - \bar{m}_c, 0\}. \tag{59}$$

Whenever the premium is positive, total remuneration equals the applicable value. If the market value exceeds it, the premium is zero and the project retains market revenue. Fixed-tariff projects instead receive the applicable feed-in tariff directly.

Using expected annual production q_{jcgt} from Equation (54), the private lifetime operating value used in the entry model is

$$V_{jcg} = \sum_{t=1}^{20} \beta^{t-1} q_{jcgt} \frac{s_{jcgt}}{100}, \qquad \beta = 0.95. \tag{60}$$

The twenty-year horizon is common across cohorts. It standardizes the investment-value object and is distinct from the government-expenditure accounting used in the counterfactual budget below.

8.2.3 Offshore remuneration

Offshore wind is not estimated in the entry model and is held fixed in all subsidy counterfactuals, but I construct its revenue consistently for the descriptive data. The historical offshore regimes do not use the onshore quality-factor correction. Instead, older statutory schemes extend the high-payment period for projects farther from shore and in deeper water. In the regimes for which the extension applies, months of additional high remuneration are constructed from distance d_j in nautical miles and water depth h_j in meters as

$$E_j = 0.5 \lfloor \max(d_j - 12, 0) \rfloor + 1.7 \lfloor \max(h_j - 20, 0) \rfloor, \tag{61}$$

subject to the statutory regime-specific eligibility conditions.

The main legacy schedules are summarized in Table 14. The EEG 2012 and EEG 2014 compressed options front-load support; later projects move to project-specific auction values under the WindSeeG/EEG market-premium system. For auctioned projects, a project-specific award is used when observed and otherwise the identified auction round is represented by its capacity-weighted average successful award value.

Expected offshore generation uses the hourly ERA5 procedure described above rather than the old mean-wind/Rayleigh approximation. Directly marketed offshore projects use the offshore-specific market-value series, with the same trailing five-year expectation rule as in Equation (58). Offshore capacity and its hourly production profile are held fixed when comparing the onshore subsidy regimes.

Table 14. Summary of offshore remuneration regimes used in the revenue construction

Entry period	Main payment values (ct/kWh)	Treatment
2009–2011	15.00 initial; 3.50 base	EEG 2009; high-payment duration may be extended by distance/depth.
2012–Jul. 2014	19.00 compressed; 15.00 extension; 3.50 base	EEG 2012 compressed schedule when applicable.
2014–2017	19.40 compressed; 15.40 standard/extension; 3.90 base	EEG 2014, subject to transition rules for late-2014 projects.
2018–2019	18.40 compressed; 14.90 standard/extension; 3.90 base	EEG 2014 degression.
2020	13.90 standard; 3.90 base	Legacy statutory regime where applicable.
2021–2023	project auction value	WindSeeG/EEG market premium; no onshore-style quality-factor multiplier.

8.3 Representative Hours

The dispatch model uses 1,000 representative hours selected from the 8,760 hours of 2023. I use k-medoids so that each representative observation is an actual hour rather than a synthetic average. This preserves coherent joint realizations of demand, wind, imports, and other system conditions.

For each TSO r, modeled domestic demand is $\widetilde{D}_{rh}$ as defined in the main text: observed load, including pumped-storage charging, net of imports. Let R_{rh} denote the same fixed non-wind renewable generation used in the dispatch model. The two clustering variables for each TSO are pre-wind residual demand

$$X^D_{rh} = \widetilde{D}_{rh} - R_{rh} \tag{62}$$

and observed gross wind

$$X^W_{rh} = W^{obs,on}_{rh} + W^{obs,off}_{rh} + \kappa^{hist}_{rh}, \tag{63}$$

where historical curtailment κ^{hist}_{rh} is added back only to reconstruct the underlying wind state. It is not imposed on the subsequent dispatch problem.

With four TSOs, the hourly clustering vector contains eight variables,

$$X_h = (X^D_{1h}, \ldots, X^D_{4h}, X^W_{1h}, \ldots, X^W_{4h})'. \tag{64}$$

Each component is standardized over the full year to zero mean and unit variance. I then apply partitioning around medoids (PAM) with Euclidean distance and 1,000 medoids. If representative hour h represents n_h full-year hours, its weight is

$$\omega_h = \frac{n_h}{8760}, \qquad \sum_{h \in \mathcal{H}} \omega_h = 1, \tag{65}$$

which is the same weighting used in Equation (35). All subsidy and grid scenarios use the identical medoids and weights. Annual quantities are recovered by multiplying each medoid outcome by its represented-hour count n_h and summing across medoids.

Table 15. Distributional fit of representative-hour clustering targets

Feature	Full mean (GW)	Rep. mean (GW)	Full SD (GW)	Rep. SD (GW)	Full p5 (GW)	Rep. p5 (GW)	Full p50 (GW)	Rep. p50 (GW)	Full p95 (GW)	Rep. p95 (GW)
Pre-wind residual load: 50Hertz	8.50	8.49	3.28	3.25	2.84	2.89	8.51	8.48	13.72	13.61
Pre-wind residual load: TenneT	9.16	9.14	4.74	4.71	1.77	1.77	8.72	8.60	17.30	17.22
Pre-wind residual load: Amprion	16.26	16.24	4.97	4.93	8.58	8.74	16.20	16.13	24.41	24.34
Pre-wind residual load: TransnetBW	4.78	4.77	2.25	2.23	1.39	1.42	4.54	4.51	8.69	8.69
Gross wind state: 50Hertz	5.02	5.02	4.22	4.22	0.38	0.40	3.74	3.66	13.71	13.77
Gross wind state: TenneT	8.58	8.58	6.44	6.42	0.87	1.00	7.04	7.07	20.56	20.51
Gross wind state: Amprion	3.02	3.00	2.50	2.49	0.18	0.22	2.32	2.31	8.08	8.15
Gross wind state: TransnetBW	0.45	0.45	0.41	0.41	0.01	0.01	0.33	0.33	1.30	1.31

Notes: Full refers to all 8,760 hours of 2023. Rep. reports the mean, standard deviation, 5th percentile, median, and 95th percentile of the 1,000 medoids, weighted by the number of source hours assigned to each medoid. Pre-wind residual load equals gross observed load including storage charging minus net imports and non-wind renewable generation. Gross wind state equals observed onshore and offshore wind injection plus observed curtailment.

Table 15 shows that the represented-hour weighting preserves the central tendencies of the eight clustering variables closely and also captures their broad dispersion and tails. As modeling

congestion requires to capture the tails well the good fit in this regard is crucial. The remaining differences in some quantiles are the cost of reducing 8,760 realized hours to 1,000 actual medoids rather than synthetic average states.

8.4 Transmission Network and Line Capacity

The network exposition follows the spatial electricity-network formulation in Bohn et al. (1984) and the incidence-matrix representation used by Arkolakis and Walsh (2023). For the full proof of the derivation of the linear approximation to the full alternating current grid model please refer to those two references. The dispatch network has the four TSO regions as nodes, but physical lines crossing TSO boundaries are retained separately rather than collapsed to one bilateral transfer limit. Parallel lines therefore remain distinct constraints. Let A be the line–node incidence matrix after omitting a reference node and let Ω be the diagonal matrix of line admittances. The flow mapping used in the main text is

$$H = \Omega A (A' \Omega A)^{-1}, \qquad Z^s_h = H I^s_{-r_0,h}, \tag{66}$$

where $I^s_{-r_0,h}$ contains the TSO injections I^s_{rh} from Equation (21) after omitting the reference node r_0. For line ℓ,

$$\Omega_\ell = \frac{1}{\sqrt{R^2_\ell + X^2_\ell}}. \tag{67}$$

Line limits follow a St. Clair-type loadability rule. When the observed reactance and susceptance imply a plausible surge impedance, I use

$$\mathcal{Z}^{surge}_\ell = \sqrt{\frac{X_\ell}{B_\ell 10^{-6}}}, \tag{68}$$

provided the resulting value lies between 150 and 600 ohms. Otherwise, the surge-impedance benchmark is 250 ohms for lines at or above 300 kV, 300 ohms for 200–299 kV, 350 ohms for 100–199 kV, and 400 ohms below 100 kV. Surge-impedance loading is

$$SIL_\ell = \frac{V^2_\ell}{\mathcal{Z}^{surge}_\ell}, \tag{69}$$

and the line limit is

$$\overline{Z}^{SC}_\ell = m(L_\ell) SIL_\ell, \tag{70}$$

where the St. Clair multiplier $m(L_\ell)$ declines with line length, from roughly 3 for short lines toward 0.6 at 600 miles.

Very short line segments require regularization because near-zero electrical lengths can generate extreme admittances and artificial bottlenecks after aggregating the grid to four TSO nodes. I impose a minimum electrical length of 5 km. For shorter lines, or for lines with missing or non-positive

electrical parameters, resistance and reactance are bounded using median per-kilometer values for valid lines in the same voltage class. Susceptance is made consistent with the voltage-class surge-impedance benchmark when the raw X/B combination is implausible. If a line shorter than 5 km has an observed current rating, its capacity instead uses the three-phase thermal limit

$$\overline{Z}_{\ell}^{I} = \frac{\sqrt{3} V_{\ell} I_{\ell}}{1000}. \tag{71}$$

This prevents short substation connectors from dominating the reduced network mechanically while preserving separate physical line constraints.